Bacterial Community Shift and Coexisting/Coexcluding Patterns Revealed by Network Analysis in A Bioreduced Uranium Contaminated Site after Reoxidation

Li, B., Wu, W-M., Watson, D. B., Cardenas, E., Chao, Y., Phillips, D., Mehlhorn, T., Lowe, K., Kelly, S. D., Li, P., Tao, H., Tiedje, J. M., Criddle, C. S., & Zhang, T. (2018). Bacterial Community Shift and Coexisting/Coexcluding Patterns Revealed by Network Analysis in A Bioreduced Uranium Contaminated Site after Reoxidation. *Applied and Environmental Microbiology*, *84*(9), [e02885-17]. https://doi.org/10.1128/AEM.02885-17

Published in:
Applied and Environmental Microbiology

Document Version:
Peer reviewed version

Bacterial Community Shift and Coexisting/Coexcluding Patterns Revealed by Network Analysis in A Bioreduced Uranium Contaminated Site after Reoxidation

Bing Li[1,2,3,4], Wei-Min Wu[2#], David B. Watson[3], Erick Cardenas[5], Yuanqing Chao[1,3], D. H. Phillips[6], Tonia Mehlhorn[3], Kenneth Lowe[3], Shelly D. Kelly[7], Pengsong Li[2,3,8], Huchun Tao[2,8], James M. Tiedje[5], Craig S. Criddle[2], Tong Zhang[1#]

[1] Department of Civil Engineering, The University of Hong Kong, Hong Kong, China
[2] Department of Civil and Environmental Engineering, William & Cloy Codiga Resource Recovery Research Center, Center for Sustainable Development and Global Competitiveness, Stanford University, Stanford, CA 94305-4020
[3] Environmental Sciences Division, Oak Ridge National Laboratory, P.O. Box 2008, Oak Ridge, Tennessee 37831
[4] Key Laboratory of Microorganism Application and Risk Control of Shenzhen, Graduate School at Shenzhen, Tsinghua University, China
[5] Center for Microbial Ecology, Michigan State University, East Lansing, Michigan 48824
[6] Queen's University of Belfast, School of Natural and Built Environment, Belfast, Northern Ireland, UK.
[7] EXAFS Analysis, Bolingbrook, IL 60440, USA
[8]Peking University Shenzhen Graduate School, School of Environment and Energy, Key Laboratory for Heavy Metal Pollution Control and Reutilization, Shenzhen 518055, China

Running title:

Bacterial Community Profiles and Co-occurrence

Corresponding authors:

Dr. Wei-Min Wu
Phone: 1-650-724-5310 Fax：1-650-725-3164 Email: billwu@stanford.edu
Address： Department of Civil & Environmental Engineering, 473 Via Ortega, Stanford, CA94305-4020, USA

Prof. Tong Zhang
Phone: 852-28578551 Fax：852-25595337 Email: zhangt@hku.hk
Address：HW6-31, Composite Building, Dept. of Civil Engineering, The University of Hong Kong, Pokfulam Road, Hong Kong

ABSTRACT:

A site in Oak Ridge, Tennessee, USA, has sediments that contain >3% iron oxides and is contaminated with uranium (U). The U(VI) was bioreduced to U(IV) and immobilized *in situ* through intermittent injections of ethanol. Then it was allowed to reoxidize via the invasion of low-pH (3.6–4.0), high-nitrate (up to 200 mM) groundwater back into the reduced zone for 1,383 days. To examine the biogeochemical response, high-throughput sequencing and network analysis were applied to characterize bacterial population shifts, as well as co-occurrence and co-exclusion patterns among microbial communities. Paired t-test indicated no significant changes of α-diversity for the bioactive wells. However, both nonmetric multidimensional scaling and analysis of similarity confirmed a significant distinction in the overall composition of the bacterial communities between the bioreduced and the reoxidized sediments. The top 20 major genera accounted for >70% of the cumulative contribution to the dissimilarity in the bacterial communities before and after the groundwater invasion. *Castellaniella* had the largest dissimilarity contribution (17.7%). For the bioactive wells, the abundance of the U(VI)-reducing genera *Geothrix*, *Desulfovibrio*, *Ferribacterium*, and *Geobacter* decreased significantly, whereas the denitrifying *Acidovorax* abundance increased significantly after groundwater invasion. Additionally, seven genera, i.e., *Castellaniella, Ignavibacterium, Simplicispira, Rhizomicrobium, Acidobacteria Gp1, Acidobacteria Gp14* and *Acidobacteria Gp23* were significant indicators of bioactive wells under

reoxidation stage. Canonical correspondence analysis indicated that nitrate, manganese and pH affected mostly the U(VI)-reducing genera and indicator genera. Co-occurrence patterns among microbial taxa suggested the presence of taxa sharing similar ecological niches or mutualism/commensalism/synergism interactions.

IMPORTANCE:

High-throughput sequencing technology in combination with a network analysis approach were used to investigate the stabilization of uranium and the corresponding dynamics of bacterial communities at field conditions with regard to the heterogeneity and complexity of the subsurface over the long term. The study also examined diversity and microbial community composition shift, the common genera and indicator genera before and after long-term contaminated groundwater invasion, and the relationship between the target functional community structure and environmental factors. Additionally, deciphering co-occurrence and co-exclusion patterns among microbial taxa and environmental parameters could help predict potential biotic interactions (cooperation/competition), shared physiologies, or habitat affinities, thus, improving our understanding of ecological niches occupied by certain specific species. The above findings offer new insights into compositions of and associations among bacterial communities and serve as a foundation for future bioreduction implementation and monitoring efforts applied to uranium-contaminated sites.

INTRODUCTION

Area 3 at the U.S. Department of Energy's (DOE's) Oak Ridge Field Research Center (ORFRC) in Oak Ridge, Tennessee, is one of the most-studied sites for *in situ* uranium bioremediation and immobilization (1-6). The sediments in this area were highly contaminated with uranium (200–1,000 mg/kg) (7). During *in situ* field studies, a hydraulic control system combined with intermittent ethanol injection successfully achieved the reduction of the U(VI) concentration in groundwater from 5 μM to levels below the U.S. Environmental Protection Agency's maximum allowable contaminant level for drinking water (0.126 μM) over a 2-year period (3,6). The bioreduction tests in Area 3 at ORFRC were terminated on December 19, 2008. After that, the hydraulic control system was discontinued, and a natural influx of outside contaminated groundwater with high nitrate concentrations (>200 mM) and low pH (3.6–4.0) invaded the previously bioreduced zone (8).

A proper bacterial community structure has been suggested as one of the key issues for the long-term stabilization of uranium by in situ bioreduction (9). In the previous investigation under bioreduction conditions, bacterial surveys of sediments and groundwater detected genera belonging to U(VI)-reducing members, such as *Desulfovibrio, Geobacter, Desulfosporosinus, Anaeromyxobacter* and *Acidovorax* (3-4,10). Ethanol, nitrate, sulfide, and uranium were correlated with specific bacterial populations, and that the engineering control of dissolved oxygen and delivered electron donor sources were significant in explaining the bacterial community variability at Area 3 (4). As a result of the termination of ethanol injection and the invasion of outside groundwater, different niches with gradients of nitrate and pH were created during this period. Therefore, we expected that the bacterial community would shift greatly compared with the community found in the area during the bioremediation period. During short-term reoxidation tests, bacterial community structure and nitrate played an important role in U(IV) oxidation (1,11). In column experiments with sediment samples from a former uranium processing site at Old Rifle, Colorado, nitrate addition stimulated U(IV) reoxidation and remobilization in previously bioreduced sediments (12,13). These previous short-term studies provided somewhat valuable information about the stabilization of uranium and the corresponding dynamics of bacterial communities. Nevertheless, they did not reconstruct field conditions with regard to the heterogeneity and complexity of the subsurface over the long term. Moreover, the results obtained from short-term tests lasting for dozens of days could not reflect the actual situation in the long term. In addition, currently little is known about the effect of groundwater invasion on bacterial community diversity/composition, which plays a crucial role in U(IV) reoxidation/sequestration after a long-term groundwater intrusion.

Most previous studies describing and comparing the structure of microbial communities mainly focused on the total numbers of taxa or unique lineages found in individual samples (i.e., α-diversity), the relative abundances of individual taxa or lineages, and the extent of phylogenetic or taxonomic overlap among communities or community categories (i.e., β-diversity) (14). In contrast, far less attention has been focused on using a network analysis approach to explore the direct or indirect interactions among microbial taxa coexisting/co-excluding in environmental samples (14-16). Network analysis of taxon co-occurrence or co-exclusion patterns could offer new insights into the structures of complex microbial communities, which could complement and expand on the information provided by the more standard suites of analytical approaches. In this study, we used high-throughput sequencing technology in combination with a network analysis approach to characterize the bacterial community structure and co-occurrence/co-exclusion patterns among genera at Area 3 of the ORFRC site during the bioreduction and reoxidation stages. The questions we wished to address are summarized as follows:

(1) Do the diversity and microbial community composition shift significantly after contaminated groundwater invasion?

(2) Which genera are common and which genera could act as the indicator genera before and after long-term groundwater invasion?

(3) What is the relationship between the target functional community structure and environmental factors?

(4) How can the co-occurrence and co-exclusion patterns among microbial taxa and environmental parameters be deciphered?

MATERIALS AND METHODS

Site description and sampling

Groundwater and sediment samples were retrieved from Area 3 of the DOE ORFRC on October 5, 2005 (after 775 days of bioremediation, named "bioreduction stage") and October 3, 2012 (after 1,383 days of exposure to the invasion of contaminated groundwater, named "reoxidation stage"). During the bioreduction stage, a hydraulic controlled system was built to inject ethanol intermittently into the subsurface as an electron donor and to control groundwater flow as well (3). An outer groundwater recirculation loop (extraction at well FW103, injection at well FW024) kept an inner loop (extraction at well FW026, injection at well FW104) from infiltration by highly contaminated groundwater from outside (Figure S1). The downgradient well of FW105, was used to monitor the impact of the treatment on the geochemistry of groundwater that transferred to the downgradient (17,18). Multilevel sampling (MLS) wells FW100, FW101, and FW102 were utilized to monitor hydrogeology and remediation performance along seven different depths. Injection and extraction wells were 14.6 m belowground, and screens were placed between 11.28 and 13.77 m.

Samples were collected from MLS wells at 15.24, 13.7, 12.19, and 10.67 m belowground for levels -1, -2, -3, and -4, respectively (3). Judged by the tracer recovery, FW026, FW104, FW101-2, FW101-3, FW102-2 and FW102-3 were considered to be bioactive wells where the U(VI) bioreduction predominantly occurred. During the reoxidation stage, the hydraulic control system was discontinued, and a natural influx of contaminated groundwater invaded the bioremediation sites. The sampling procedure was described in our previous studies (3,19). Briefly, sediments were collected from each well using a polyvinyl chloride surge block to draw the sediments surrounding the well screen into the well, and were then pumped into glass bottles under a nitrogen gas phase. The sediments were later separated from the slurry by centrifugation and stored at −80°C until DNA extraction.

Analytical methods

Analytical methods were the same to those described previously (1, 3). Anions including nitrate and sulfate were determined using an ion chromatograph (Dionex DX-120, Sunnyvale, CA, USA). Metals were analyzed by inductively coupled plasma mass spectrometry (Perkin-Elmer ELAN 6100 spectrometer). N_2O was detected by an SRI model 8610-0072 gas chromatograph with a TCD detector (1). Ammonium and ammonia concentrations were determined by Activation Laboratories, Ltd, Ontario, Canada.

DNA extraction, PCR amplification, and 454 pyrosequencing

The DNA extraction was conducted using the FastDNA® SPIN Kit for Soil (MoBio Inc., CA, USA) and the DNA concentrations, as well as purity, were detected using the NanoDrop® ND-1000 (NanoDrop Technologies, Wilmington, DE). DNA was amplified with the forward primer 338F (5'-ACTCCTACGGGAGGCAGCAG-3') and with the reverse primer 802R (5'-TACNVGGGTATCTAATCC-3') targeting the V3–V4 regions (~465 nucleotides) of the 16S rRNA genes (20). Each polymerase chain reaction (PCR) was conducted in a 50 μl reaction system using a MightyAmp polymerase (TaKaRa, Otsu, Japan) and an i-Cycler (BioRad, Hercules, CA, USA) under the following PCR conditions: initial denaturation at 94°C for 5 min; 30 cycles at 94°C for 50 s, 50°C for 45 s, and 72°C for 90 s; and a final extension at 72°C for 5 min. The PCR products were purified and quantified using the NanoDrop® ND-1000 and then mixed in equal amounts for the subsequent pyrosequencing on a Roche 454 FLX Titanium platform (454 Life Sciences, Roche) at the Genome Research Centre of The University of Hong Kong, Hong Kong.

Sequence processing

The raw sequencing data from 454 pyrosequencing were processed using the QIIME pipeline v1.7.0 (21). Briefly, the raw sequences were first parsed into different samples with barcode primers removed, denoised by Denoiser (22), and chimera-checked using ChimeraSlayer (23) to yield error-free reads. Then the normalization of the effective sequences was conducted by randomly extracting 5,364 clean sequences from each sample dataset (except for one sample titled FW100-2-R, which had effective sequences of 1,970) to fairly compare all samples at the same sequencing depth (Table S1). The normalized sequences from all samples were clustered into operational taxonomic units (OTUs) using the Uclust algorithm (closed-reference OTU picking protocol) at identity thresholds of 0.97 (24), which approximately corresponds to the taxonomic level of species for bacteria. Taxonomic classification of the effective sequences of each sample was carried out individually, using the RDP classifier (25) with an 80% confidence level. Among these 30 datasets, 14 datasets of the samples collected from the bioreduction stage were used in our previous study investigating the significant association between sulfate-reducing bacteria and uranium-reducing bacterial communities (3).

Statistical and network analysis

The α-diversity analysis including richness (OTUs, Chao 1, and ACE) and diversity index (Shannon index) at a cutoff level of 3% was conducted using QIIME. Buzas and Gibson's evenness was calculated using PAST software (version 2.14 for Windows) on the basis of the OTU table generated by QIIME (26). Distances between bacterial communities (at 3% cutoff-OTU level) in different samples were calculated using the weighted UniFrac and unweighted UniFrac beta-diversity metric via QIIME. Nonmetric multidimensional scaling (NMDS) was used to visualize the bacterial community differences at both the 3% cutoff-OTU level and genus level obtained from the RDP taxonomic results. Cluster analysis of bacterial profiles in the bioactive wells under the bioreduction and reoxidation stages was also conducted based on the Bray-Curtis distance calculated from the matrix of genus relative abundance using PAST software. Additionally, canonical correspondence analysis (CCA), analysis of similarity (ANOSIM), and similarity of percentages analysis (SIMPER) were performed using PAST software. To identify the specific genera that characterize each of the environments, we used Indicator Species Analysis run in R (version 2.14.0) (27), using the package *labdsv* (http://ecology.msu.montana.edu/labdsv/R) and test *indval* (28). Network analyses were conducted in the R environment using the VEGAN (29), igraph (30), and Hmisc packages (31). Network visualisation was carried out on the interactive platform of Gephi (32). The detailed analysis procedure is summarized in S1 (Supplementary Material).

Accession numbers

All the 454 pyrosequencing sequences were deposited in the NCBI Sequence Read Archive under accession number PRJNA338649.

RESULTS AND DISCUSSION

Changes in geochemistry after reoxidation

After long-term invasion of contaminated groundwater for 1,383 days (3.78 years), the geochemistry in all wells had changed significantly, especially with regard to decline in pH, increase in oxidation / reduction potential (ORP) from near -200 mV or lower (under conditions in the presence of sulfide) to the 200-300 mV range, increase in anions (nitrate, sulfate and chloride), and metals (U, Al, Ca, Mg, Mn, etc) concentrations (Table 1). Sulfite disappeared in the test area. Sediment samples collected from bioactive monitoring wells changed from dark or greenish in color to yellow, indicating they underwent oxidation. The rapid decrease in pH from above 5.5 to 4.2 or lower was observed in wells located near the boundary of the biotreatment zone, such as FW100-2 and 100-3. The pH in all wells located in the previous bioactive zone (wells FW101-2 and FW101-3) declined to below 5.0 with the increase in nitrate concentrations from near zero to significantly high levels (60 to 100 mM). However, the pH in the previous bioactive wells FW102-2 and FW102-3 declined slightly with a significant increase of nitrate (58.7 and 27.0 mM). Low levels of ammonium (but no ammonia) were determined in all previous active wells at 0.083-0.194 mM. However, similar levels of ammonium were also determined in downgradient well FW105 (0.213 mM) and another monitoring well FW106 (0.182 mM) which is separated from the previous test zone. After the long-term invasion, the aqueous U concentrations increased in all wells. The U content in the sediment samples from the previously bioreduced zone (FW101-2, FW101-3, FW102-2 and FW102-3) remained high or even higher than before, suggesting strong uranium sequestration (Table 1). Mn concentrations were increased significantly in all wells. Other non-bioreduction/oxidation related cations (Mg, Ca and Al) and chloride also increased, likely due to invasion of around contaminated groundwater. The DO concentrations in all wells remained low (<0.3 mg/L, Table 1), since the groundwater in Oak Ridge Field Research Center Areas 2 and 3 contains low DO (33). The significant increase in ORP (Table 1) in all monitoring wells was likely due to the groundwater had more new species (especially nitrate) to gain electrons.

Overall bacterial community shift before and after long-term groundwater invasion

Analyses for α-diversity (OTUs, Chao 1 and ACE), evenness (Buzas and Gibson's evenness), and diversity index (Shannon index) were conducted at the same sequencing depth of 5,364 sequences excluding one sample having 1,970 effective sequences (Table S1). To investigate the effect of the long-term (1383 days) groundwater invasion on α-diversity, FW101-2, FW101-3, FW102-2, FW102-3, FW104, and FW026, the bioactive wells with high bioactivity where U(VI) reduction occurred during the in situ uranium bioremediation process (3), were selected for a comparison of richness, evenness, and diversity index between the bioreduction stage (data published on reference

5) and reoxidation stage (data in the present study), i.e., 484–982 vs. 418–848 (OTUs), 876–1978 vs.735–1840 (Chao 1), 918–1974 vs. 781–2022 (ACE), 0.77–2.96 vs. 0.27–2.03 (evenness), and 5.98–7.98 vs. 4.78–7.53 (Shannon index), respectively. Paired *t*-tests indicated that there was no significant difference (P-value = 0.14–0.47) in α-diversity before and after the long-term invasion of groundwater for these bioactive wells.

As we hypothesized previously, significant differences in the bacterial community compositions were observed before and after the groundwater invasion due to the impacts of changes in geochemical conditions. Thirty samples formed two distinct clusters, in accordance with the bioreduction and reoxidation stages, on the NMDS plot of the bacterial community compositions (at the genus level) of all the selected wells (Figure 1). Using OTU abundance, a similar clustering pattern was confirmed by both weighted and unweighted UniFrac (Figure S2), revealing that the clusters were influenced mainly by the bioreduction and reoxidation stages. ANOSIM was conducted to further test whether significant differences in community composition occurred after the long-term invasion of groundwater. Results suggest that there is a significant distinction in the overall composition of the microbial communities between the bioreduction and reoxidation stages (R_{ANOSIM}=0.59, P=0.0001). In addition, the coordinate position shift of each specific sample in Figure S3 reflects the obvious variation of microbial community after the long-term invasion of groundwater. All the above results explicitly confirmed our hypothesis.

Figure 1

SIMPER was used to determine the relative contribution of individual genus to the dissimilarity between the two clusters. The average Bray–Curtis dissimilarity and the contribution of each genus to the total dissimilarity between communities before and after groundwater invasion were calculated, and the top 20 major genera largely responsible for the microbial community shift (>70% contribution to cumulative dissimilarity) are summarized in Table 2. Among them, *Castellaniella* had the largest dissimilarity contribution (17.7%), followed by *Rhodanobacter* (10.9%), *Desulfosporosinus* (5.81%), *Sulfuricurvum* (5.34%), *Clostridium-sensu-stricto* (3.45%), *Mycobacterium* (3.45%), *Simplicispira* (3.23%), and *Desulfovibrio* (3.12%).

Moreover, analysis of the bioactive wells (FW101-2, FW 101-3, FW 102-2, FW 102-3, FW 104 and FW 026) found that they were much similar to one another at the bioreduction stage than at the reoxidation stage (Figure 1 and Figure S2). The closer grouping pattern at the bioreduction stage revealed the similar bacterial community compositions in these wells due to the strong environmental stresses applied during bioremediation, whereas the divergence in distribution at the reoxidation stage suggested the long-term invasion of groundwater led to the obvious dissimilarity.

Figure 2

Figure 2(a) illustrates the abundance of different phyla in all samples at both the bioreduction and reoxidation stages. *Proteobacteria* was the most abundant phylum in almost all samples except for FW100-2-R, FW026-R, FW104-O, and FW101-2-O. This finding is similar to the analytical results for bacterial communities in acid mine drainage (34), unconfined aquifer (35), sediment (36), and soil (37) in which *Proteobacteria* was also the most dominant community. The abundances of *Proteobacteria* at the bioreduction and reoxidation stages, respectively, ranged from 17.9% to 70.4% (average abundance of 38.6%) and 20.5% to 89.7% (average abundance of 58.0%). In addition, paired *t*-test indicated that *Proteobacteria* abundance was significantly higher (P-value = 0.008) at the reoxidation stage. The other dominant phyla in bioactive wells at the bioreduction stage (FW101-2-R, FW101-3-R, FW102-2-R, FW102-3-R, FW104-R, and FW026-R) were *Acidobacteria* (10.6–33.2%), *Firmicutes* (5.1–15.7%), *Chlamydiae* (4.8–17.1%) and *Actinobactera* (2.3–8.3%); while *Acidobacteria* (4.3–60.6%), *Bacteroidetes* (1.0–18.0%) and *Firmicutes* (0.8–46.4%) were the abundant phyla apart from *Proteobacteria* in bioactive wells at reoxidation stage (FW101-2-O, FW101-3-O, FW102-2-O, FW102-3-O, FW104-O and FW026-O). Many members of *Acidobacteria* are known to prefer to acidic conditions. This might be the potential reason why *Acidobacteria* is predominant in bioactive wells at reoxidation stage with low pH groundwater invasion. It is interesting that in the sample of FW101-2-O, *Firmicutes* was the most dominant phylum, accounting for as much as 46.5% of the population, much more than in the counterpart FW101-2-R (14.7%). Not only the abundance but also the composition of *Firmicutes* altered drastically after the long-term groundwater invasion (Figure 2(b) and Figure S5). The detailed discussion of the bacterial community composition is summarized in S2 (Supplementary Material).

Common genera before and after long-term groundwater invasion

Figure 3 illustrates the abundance of the 77 major genera (>0.5% in at least one sample) belonging to 14 different phyla in the 30 sediment samples before and after long-term groundwater invasion. Major genera with occupancies >80% of all samples and average abundances >0.1% were defined as common genera in the present study. Among these 77 major genera, 36 genera belonging to 10 different phyla were classified as common genera. The common genera, including *Sphingomonas, Gp3, Geothrix, Gp1, Subdivision3_genera_incertae_sedis, Gemmatimonas, Gp16, Mycobacterium, Simplicispira, Clostridium-sensu-stricto,* and *Rhodanobacter* were universal and occurred in all 30 sediment samples with average abundances ranging from 0.51% (*Sphingomonas*) to 10.6% (*Rhodanobacter*). It is noteworthy that *Gp1*, *Gp3* and *Gp16* belong to the phylum of *Acidobacteria* while *Subdivision3_genera_incertae_sedis* belong to the phylum of *Verrucomicrobia.*

Figure 3

According to previous studies (3-4,10,38), reduction of U(VI) was facilitated by a number of different genera, including *Desulfovibrio, Geobacter, Anaeromyxobacter, Desulfosporosinus, Acidovorax, Geothrix, Ferribacterium, Clostridium, Desulfotomaculum,* and *Shewanella*. Additionally, U (VI) reduction cannot be attributed to a single group, and is carried out by several different bacteria as well as abiotic reduction by Fe(II) compounds after bioreduced condition is established (39-40). Among these known U(VI)-reducing genera, eight genera (excluding *Acidovorax* and *Ferribacterium*) were common genera. In the bioactive wells, the abundance of *Geothrix*, *Desulfovibrio, Ferribacterium* and *Geobacter* decreased significantly after the long-term groundwater invasion, whereas the abundance of *Acidovorax* increased significantly (P-value <0.05). However, the abundances of *Desulfosporosinus* and *Anaeromyxobacter* remained abundant, averaging 3.15%–11.7% and 0.57%–0.78%, respectively. The abundances of *Clostridium-III, Clostridium-sensu-stricto, Clostridium-XI,* and *Clostridium-XIVa* also showed no significant variation. We examined whether the average abundances of these U(VI)-reducing genera varied significantly in samples from bioactive wells versus inactive wells. At the bioreduction stage, the average abundances of *Geothrix, Desulfosporosinus, Anaeromyxobacter, Desulfovibrio, Geobacter,* and *Ferribacterium* in bioactive wells were significantly higher (P-value < 0.05, Table S3) than those in inactive wells, whereas the abundances of *Acidovorax* and *Clostridium* remained unchanged in both bioactive and inactive wells. The metabolic functions of the former group were clearly related to metal (Fe, U) and sulfate reduction, whereas the functions of the latter two organisms likely depended more on nitrate metabolism than on metal reduction. Nevertheless, at the reoxidation stage, only *Desulfosporosinus* was more abundant in bioactive wells, and all the other U(VI)-reducing genera abundances exhibited no significant difference between bioactive wells and inactive wells (Table S3). This result demonstrates that the significantly differential abundance of U(VI)-reducing bacterial communities established in samples from bioactive versus inactive wells during the bioremediation process abated greatly after the long-term groundwater invasion.

Geothrix, an Fe(III)-reducing bacterial member of the *Acidobacteia*, has been widely detected in ORFRC sediment and groundwater with bioreduced U(VI) in previous studies (1,4,10,41-42). Although no direct evidence has shown that it reduced U(VI) to U(IV) in a pure culture (10,41,43), *Geothrix* was speculated to contribute to U(VI) reduction indirectly via its known ability to produce bioreduced humic acids or reduced iron compounds, which are capable of reducing U(VI) to U(IV) abiotically (39,40,44-45). A detailed functional discussion of other U(VI)-reducing genera, including *Geobacter, Anaeromyxobacter, Acidovorax*, *Desulfovibrio, Desulfosporosinus, Ferribacterium,* and *Clostridium* is summarized in S3 (Supplementary Material). It should be pointed out that the proposed functions of these genera are actually their potential functions obtained based on literatures review. We speculate that some bacterial strains belonging to the genus might possess such functions although not all the strains belonging to the genus have the same function.

Indicator genera for bioactive wells

Microbial diversity, abundance, and composition change along environmental gradients. Understanding the nature of these changes might facilitate to identify a set of environmental conditions characteristic to specific groups of taxa. Finally, these relationships could be used to find microbial indicators that would represent specific environments and help predict microbial community responses to environmental conditions (46). During the long-term groundwater invasion, both the geochemical conditions and microbial communities of the bioactive wells changed greatly (Table 1, Figure 1 and Figure 3). We therefore expanded on the indicator species analysis at both the bioreduction and reoxidation stages to evaluate the relationship between these indicator species and the stability and mobility of the preciously reduced uranium.

The bacterial profiles of the bioactive well samples collected at the reoxidation and bioreduction stages formed two distinct clusters, Cluster I and Cluster II, respectively (Figure S8). Indicator species approach was used on the resulting clustering topology to find groups representing specific groups of samples (28). Eleven genera were significant indicators of Cluster II (Table 3). Three of these genera, i.e., *Desulfovibrio*, *Ferribacterium* and *Geobacter* belonged to known U(VI)-reducing genera. *Desulfovibrio* and *Geobacter* can also perform dissimilatory nitrate reduction to ammonia (47-49).These results were consistent with the findings in high-bioactivity wells reported by Cardenas et al. (3). Cluster I, with seven significant indicators (*Castellaniella, Ignavibacterium, Simplicispira, Rhizomicrobium, Acidobacteria Gp1, Acidobacteria Gp14 and Acidobacteria Gp23*), did not contain indicator species from known metal or U(VI)-reducing genera (Table 3). *Castellaniella* was once characterized as the significant indicator species for inactive wells with low pH, heavy metals, and low bioactivity at the bioreduction stage. This finding was reasonable because the geochemical conditions in bioactive wells after the groundwater invasion were similar to those in inactive wells at the bioreduction stage. *Castellaniella*, a dominant denitrifier, was also previously found in the groundwater in bioremediation wells at Area 1 of the ORFRC, a location that was acidic and contaminated with uranium and nitrate (50). *Castellaniella* was isolated from that site under neutral (pH=7.5) and acidic (pH=4.5) culture conditions, indicating that it has an advantage over other denitrifiers under acidic conditions typical of the ORFRC sites. Besides Area 1 and Area 3, *Castellaniella* has also been detected in microcosm enrichments from Area 2 of the ORFRC (51).

Nevertheless, *Rhodanobacter* was not the indicator genus in the present study because its abundance was high with no significant difference in both the bioreduction stage (4.85±4.35%)

and the reoxidation stage (7.40±3.69%). *Rhodanobacter* was previously detected by 16S rRNA gene surveys (10) and by a metagenomic approach in groundwater from well FW106, an untreated control well 9.9 m southward from the treatment zone. This well had a pH of 3.6 and high levels of uranium (110–130 μM) and nitrate (38–54 mM) (52). *Rhodanobacter* was one of the microorganisms involved in acidic (pH=4.0) denitrification in soils (53). This is consistent with our study finding that a significant level of N_2O (2.0×10^4 – 4.4×10^4 ppmv) was detected in the groundwater of bioactive wells after reoxidation (pH=4.41–5.55). In addition, both Cluster I and II indicators included some poorly studied groups such as *Ignavibacterium*, *Acidobacteria Gp1*, *Acidobacteria Gp6*, *Acidobacteria Gp14*, and *Acidobacteria Gp23*. Moreover, an abundance vs occupancy plot (Figure S9) showed that some indicators, including *Parachlamydia, Arthrobacter, Desulfovibrio, Acidobacteria Gp6, Sulfuricurvum, Geobacter, Mycobacterium, Castellaniella, Simplicispira* and *Acidobacteria Gp1* displayed common taxa qualities with high relative abundance and occurrence in a high number of samples outside their indicator environment. Conversely, *Zoogloea*, *Acidobacteria Gp14* and *Acidobacteria Gp23* were more specialized to their respective environments with low occupancy.

CCA analysis-correlations between microbial communities and groundwater geochemistry

The constrained multivariate analysis CCA were used to examine and visualize the relationship between the target functional community structure (i.e., U(VI)-reducing genera and indicator genera) and environmental factors (i.e., pH, sulfate, nitrate, U(VI), Fe, etc.). Both the first and second axes were positively correlated with concentrations of DO, nitrate, Fe, Ca, Mg, Mn, U(VI), Cl^-, and sulfate while the first axes negatively correlated with pH. As summarized in Table S4, Axis 1 was dominantly represented by pH (r=-0.564), Cl^- (r=0.591), Ca (r=0.627), Mg (r=0.676), Mn (r=0.734) and nitrate (r=0.681); whereas Axis 2 was indicative of U(VI) (r=0.456), sulfate (r=0.428), and DO (r=0.348). Additionally, pH and nitrate were nearly aligned along the same line but in completely opposite directions (Figure 4). Among the U(VI)-reducing genera, *Geobacter, Geothrix, Desulfovibrio, Desulfosporosinus, Ferribacterium, Anaeromyxobacter, Clostridium-III* and *Clostridium-XI* were correlated positively with pH and negatively with higher concentrations of U(VI), Fe, DO, Mn, Mg, Ca, Cl^- sulfate and nitrate. Nevertheless, three other U(VI)-reducing genera including *Clostridium-sensu-stricto, Acidovorax*, and *Clostridium-XIVa*—were correlated negatively with pH and positively with U(VI), Fe, DO, Mn, Mg, Ca, Al, Cl^-, sulfate, and nitrate. *Ferribacterium, Desulfovibrio, Geobacter, Geothrix, Clostridium-XI, Acidovorax* and *Clostridium-XIVa* were evenly distributed along the pH and nitrate lines. This phenomenon might imply that pH and nitrate were the predominant variables leading to the significantly different abundances of these U(VI)-reducing genera before and after the long-term groundwater invasion. However, because pH and nitrate have almost contrary effects on the abundances of U(VI)-reducers, it is not easy to distinguish whether these genera are more positively affected by one variable, or negatively affected by the other, judging only by the CCA plots. Moreover, the negative correlation between *Desulfovibrio* and sulfate was meaningful in a biogeochemical context. That is, the increase in abundance of the sulfate-reducing bacteria *Desulfovibrio* corresponded with a decline in sulfate concentration (Table 1, Figure 3). Similarly, the negative correlation between *Ferribacterium*, *Geobacter,* and *Geothrix* and Fe also implies that the increase in abundance of these Fe(III) reducing-bacteria corresponded with a decline in Fe(III) concentration.

Figure 4

For the indicator genera at the bioreduction stage, all the indicator genera were correlated positively with pH and negatively with higher concentrations of U(VI), Fe, DO, Mn, Mg, Ca, Al, Cl^-, sulfate, and nitrate (Figure 4). For the indicator genera at the reoxidation stage, *Castellaniella, Ignavibacterium, Simplicispira, Rhizomicrobium, Acidobacteria GP14* and *Acidobacteria GP23* were positively correlated with U(VI), Fe, DO, Mn, Mg, Ca, Al, Cl^-, sulfate, and nitrate, whereas *Acidobacteria Gp1* were positively correlated with pH (Figure 4). This is congruent with Cardenas's finding that *Castellaniella* characterized areas with low pH and high sulfate and nitrate concentrations, whereas *Desulfovibrio*, *Anaeromyxobacter,* and *Desulfosporosinus* were indicators of U(VI) bioreduction areas with neutral pH, and low sulfate and nitrate levels (3). Previous study verified that the abundance of *Simplicispira* increased greatly as a result of nitrate addition in anaerobic sewers (54). Although *Ignavibacterium* was poorly investigated, a new isolate named

P3M-2^T belonging to *Ignavibacterium* showed the ability to reduce diverse electron acceptors such as Fe(III) (55). *Castellaniella*, the dominant *nir*K-containing denitrifier, was also previously detected with relatively high abundance in groundwater and sediments of bioremediation wells at acidic conditions and contaminated with nitrate and uranium (3,50).

Co-occurrence and co-exclusion patterns among microbial taxa and environmental parameters

The co-occurrence (Figure 5) and co-exclusion (Figure S10) patterns among bacterial taxa and environmental parameters were explored using network analysis based on strong (ρ >0.6 or ρ <–0.6) and significant (*P*-value <0.01) correlations (56). Figure 5 consists of 58 nodes (53 microbial taxa and 5 environmental parameters) and 150 edges. Some topological properties commonly used in network analysis were calculated to describe the complex pattern of interrelationships among bacterial taxa and environmental variables (S4, Supplementary Material). Based on the modularity class, the entire network could be divided into seven major modules, which are clusters of nodes interacting more among themselves than with other nodes, compared to a random association. The two largest modules, I and II, were occupied by 33 of 58 total vertices. The most densely connected node in each module was defined as the "hub" in the following statements. The co-occurring bacterial taxa of the module hubs are summarized in Table S5. Figure S10 visualizes the significantly negative correlations (79 edges) among 34 bacterial genera and 5 environmental parameters.

Figure 5

Environment–genera associations

Correlations with environmental parameters revealed putative associations among the connected taxa and particular environmental measurements. This finding could also mirror and support the CCA results between microbial communities and groundwater geochemistry from another perspective. For instance, the positive correlations between nitrate and *Simplicispira*, as well as *Castellaniella*, were also observed via the CCA approach, perhaps indicating that the increase in nitrate concentration may promote the accumulation of *Simplicispira* as well as *Castellaniella.* Likewise, the negative correlations between nitrate and *Geothrix*, *Mycobacterium, Desulfovibrio, Acidobacteria Gp6, Parachlamydia,* and *Ferribacterium,* which were reflected in the CCA results, might reveal that the invasion of nitrate-containing groundwater tended to reduce the abundances of these bacterial groups. The consistent results obtained by the CCA approach and network analysis were also commonly observed for other environmental parameter–genera associations, including the negative correlations between pH and *Clostridium-sensu-stricto*/*Clostridium-XIVa,* the positive correlation between pH and *Acidobacteria Gp6*, the negative correlations between U(VI) concentration and *Mycobacterium*/*Sulfuricurvum*/*Arthrobacter*/ *Acidobacteria Gp6*/*Ferribacterium*, the positive correlations between U(VI) concentration and *Castellaniella*/*Rhizomicrobium*, and the negative correlation between Fe concentration and *Mycobacterium*.

Genera–genera associations

In all likelihood, the co-occurrence patterns among the microbial taxa were derived from either taxa sharing similar ecological niches or a mutualism/commensalism/synergism. On the other hand, the co-exclusion patterns among different genera might reveal niche preferences for the specific taxa (non-overlapping niches) or competition (14,57). It should be pointed out that these co-occurrence or co-exclusion data alone do not allow us to separate these two possibilities, i.e., ecological niches and interaction relationships among microbial taxa (14). However, this is an example of the potential that the approach could gain clues regarding elusive but ecologically relevant microorganisms. In other words, the co-occurrence patterns and the co-exclusion patterns will improve our understanding of ecological niches occupied by unknown species and help to predict their biological functions in ecosystems. Some of the co-occurrence patterns reveal or confirm interesting ecological patterns for taxa that have been reported previously. For instance, *Geobacter* co-occurs with *Desulfovibrio* out of a relation of commensalism, in which *Desulfovibrio* uses ethanol and not acetate in the process of sulfate reduction, and the release of metabolic acetate can be used later by *Geobacter* (14). In addition, the co-occurrence pattern among three major U(VI)-reducing genera including *Ferribacterium, Geothrix* and *Geobacter* might result from their sharing similar ecological niches, instead of mutualism/commensalism/synergism, since all of them could reduce Fe (III) and U(VI) and they are competitors from this perspective. Apart from the above co-occurrence patterns, there were numerous co-occurrence relationships among different microbial taxa, including some genera not well studied, such as *OD1_genera_incertae_seids, Acidobacteria Gp6, Acidobacteria Gp4,* and *Subdivision3_genera_incertae_sedis (Verrucomicrobia)*. Although the nature of the possible interactions among these populations is unknown currently, it provides valuable clues that these distinct organisms are closely bound ecologically.

Moreover, the highly clustered and modularized structure of the positive network (Figure 5) is completely different from the unclustered and unmodularized structure of the negative network (Figure S10). The modularized structure supports the previous argument for small-world properties in microbial ecological networks, so that each genus is closely linked to all other genera in highly clustered cliques (15). Module II, Module V, and Module VI formed sub-networks; and these three modules connected with other modules only via one edge (Figure 5). For instance, Module II connected with Module I via the edge of *Acidobacteria Gp4-Brevundimonas* and Module V correlated with Module II via the edge of *Bacillus-Castellaniella*. Similarly, Module II and Module VI were bridged by the edge of *Sphingomonas-Rhizobium*. On the other hand, Module I, Module III, and Module IV were clustered more closely with each other, and more connections among these three modules were observed compared with other modules. As mentioned earlier, some of the co-occurrence patterns may represent guilds of microorganisms performing similar or complementary functions to each other, whereas others may co-occur because of shared and preferred environmental conditions. In attempting to distinguish these possibilities, it is tempting to look for positive correlations among the shared co-occurring genera of the co-occurring "hubs" in these modules. Note that if these co-occurring hubs were truly redundant (that is, ecologically identical), other taxa should have responded to both similarly, creating many shared neighbors without positive correlations. For example, the hubs of Module I and Module III, that is, *Aquicella* and *Legionella*, shared 10 co-occurring genera totally (Table S6). Among these 10 co-occurring genera, no co-occurrence among *Ferribacterium, Gemmatimonas,* and *Sediminibacterium* was observed. This pattern implies that functional redundancy presumably occurs between *Aquicella* and *Legionella* for *Ferribacterium, Gemmatimonas,* and *Sediminibacterium*. Nevertheless, it is unclear to what extent the collective suite of functions of *Aquicella* and *Legionella* overlaps (58).

For the co-exclusion patterns among the microbial taxa (Figure S10), indicator genera at the reoxidation and bioreduction stages tended to co-exclude more (12.6%) than would be expected by chance (2.4%). Additionally, U(VI)-reducing genera and indicator genera at the reoxidation stage also showed higher incidences of co-exclusion than would be expected by random association (2.8% at random vs. 5.1% observed). This might reveal the niche preference for these specific taxa (non-overlapping niches). Considering the end of the bioreduction injections of ethanol and the long-term invasion of groundwater with high concentration of nitrate and low pH, the geochemistry conditions varied greatly; thus different niches were created before and after the groundwater intrusion.

In summary, there was no significant difference in α-diversity before and after the long-term invasion of groundwater for the bioactive wells, suggesting that α-diversity is not a proper parameter to evaluate the impact of invasion of groundwater with low pH and high concentration of contaminates especially nitrate. On the other hand, both NMDS and ANOSIM confirmed a significant distinction in the overall composition of the bacterial communities between the bioreduced and the reoxidized sediments. The top 20 major genera accounted for >70% of the cumulative contribution to the dissimilarity in the bacterial communities before and after the groundwater invasion. *Castellaniella* had the largest dissimilarity contribution (17.7%). Among the ten known U(VI)-reducing genera, eight genera (excluding *Acidovorax* and *Ferribacterium*) were common genera with occupancies >80% of all samples and average abundances >0.1%. For the bioactive wells, the abundance of the U(VI)-reducing genera *Geothrix*, *Desulfovibrio*, *Ferribacterium,* and *Geobacter* decreased significantly. However, the U(VI)-reducing genera *Desulfosporosinus* and *Anaeromyxobacter* still remained abundant even after groundwater invasion, averaging 3.15%–11.7% and 0.57%–0.78%, respectively. Seven genera, i.e., *Castellaniella, Ignavibacterium, Simplicispira, Acidobacteria Gp23, Acidobacteria Gp1, Rhizomicrobium* and *Acidobacteria Gp14* were significant indicators which could represent specific environments of bioactive wells under reoxidation stage. Nitrate concentration and pH affected mostly the U(VI)-reducing genera and indicator genera. Co-occurrence patterns among microbial taxa suggested the presence of taxa sharing similar ecological niches or mutualism/commensalism/synergism interactions. Some of the co-occurrence results revealing or confirming interesting ecological patterns for taxa have been reported previously. For the possible interactions among some populations which are unclear currently, network analysis could provide valuable clues that these distinct microorganisms are closely bound ecologically. Additionally, deciphering co-occurrence and co-exclusion patterns among microbial taxa and environmental parameters could help predict potential biotic interactions (cooperation/competition), shared physiologies, habitat affinities, or their biological functions in uranium-contaminated ecosystems. The above findings offer new insights into compositions of and associations among bacterial communities and serve as a foundation for future bioreduction implementation and monitoring efforts applied to uranium-contaminated sites.

ACKNOWLEDGEMENTS

We thank Dr. Feng Guo and Dr. Feng Ju for the suggestions of data analysis.

FUNDING INFORMATION

This work was funded by the U.S. DOE Subsurface Biogeochemical Research Program under grants DOE-AC05-00OR22725 and DE-SC0006783. The pyrosequencing was partially financially supported by Hong Kong GRF (7201/11E). Drs. Bing Li, Yuanqing Chao, Huchun Tao, and Mr. Pengsong Li were visiting scholars at the Department of Civil and Environmental Engineering, Stanford University, and the Environmental Science Division, Oak Ridge National Laboratory during this study period. Dr. Bing Li was supported by an HKU postdoc scholarship and Dr. Yuanqing Chao was supported by an HKU postgraduate studentship during this study period. Huchun Tao and Pengsong Li were financially supported by the China Scholarship Council. We declare no conflict of interest.

SUPPLEMENTAL MATERIAL

Supplemental Material for this article may be found at

REFERENCES

1. Wu WM, Carley J, Green SJ, Luo J, Kelly SD, Van Nostrand J, Lowe K, Mehlhorn T, Carroll S, Boonchayanant B, Löfller FE, Watson D, Kemner KM, Zhou J, Kitanidis PK, Kostka JE, Jardine PM, Criddle CS. 2010. Effects of nitrate on the stability of uranium in a bioreduced region of the subsurface. Environ Sci Technol **44:** 5104–5111.

2. Singh G, Sengör SS, Bhalla A, Kumar S, De J, Stewart B, Spycher N, Ginn TM, Peyton BM, Sani RK. 2014. Reoxidation of biological reduced uranium: a challenge toward bioremediation. Crit Rev Environ Sci Technol 44:391–415.

3. Cardenas E, Wu WM, Leigh MB, Carley J, Carroll S, Gentry T, Luo J, Watson D, Gu BH, Ginder-Vogel M, Kitanidis PK, Jardine PM, Zhou JZ, Criddle, CS, Marsh TL, Tiedje JM..2010. Significant association between sulfate-reducing bacteria and uranium-reducing microbial communities as revealed by a combined massively parallel sequencing-indicator species approach. Appl Environ Microbiol **76:** 6778–6786.

4. Hwang CC, Wu WM, Gentry TJ, Carley J, Corbin GA, Carroll SL, Watson DB , Jardine PM , Zhou JZ , Criddle CS , Fields MW. 2009. Bacterial community succession during in situ uranium bioremediation: spatial similarities along controlled flow paths. ISME J **3:** 47–64.

5. Kelly SD, Kemner KM, Carley J, Criddle C, Jardine PM, Marsh TL, Phillips D , Watson D , Wu WM. 2008. Speciation of uranium in sediments before and after in situ biostimulation. Environ

Sci Technol **42:** 1558–1564.

6. Van Nostrand JD, Wu LY, Wu WM, Huang ZJ, Gentry TJ, Deng Y, Carley J, Carroll S, He ZL, Gu BH, Luo J, Criddle CS, Watson DB, Jardine PM, Marsh TL, Tiedje JM, Hazen TC, Zhou JZ. 2011. Dynamics of microbial community composition and function during in situ bioremediation of a uranium-contaminated aquifer. Appl Environ Microbiol **77:** 3860–3869.

7. Wu WM, Carley J, Fienen M, Mehlhorn T, Lowe K, Nyman J, Luo J, Gentile ME, Rajan R, Wagner D, Hickey RF, Gu B, Watson D, Cirpka OA, Kitanidis PK, Jardine PM, Criddle CS. 2006. Pilot-scale in situ bioremediation of uranium in a highly contaminated aquifer 1: conditioning of a treatment zone. Environ Sci Technol **40**:3978–3985.

8. Wu WM, Watson D, Li B, Phillips DH, Chao Y, Kelly SD, Mehlhorn T, Lowe K, Phillips J, Earles J, Tang G, Li P, Tao H, Chen Z, Zhang T, Criddle CS. 2014. Uranium sequestration in a previously bioreduced subsurface in response to invasion of nitrate containing groundwater. Poster presented at American Society for Microbiology 114th General Meeting, Boston, MA, USA. May 18–20, 2014.

9. Anderson RT. 2006. DOE genomics: applications to in situ subsurface bioremediation. Remediation J. 17:23–38.

10. Cardenas E, Wu WM, Leigh MB, Carley J, Carroll S, Gentry T, Luo J, Watson D, Gu BH, Ginder-Vogel M, Kitanidis PK, Jardine PM, Zhou JZ, Criddle, CS, Marsh TL, Tiedje JM. 2008. Microbial communities in contaminated sediments, associated with bioremediation of uranium to submicromolar levels. Appl Environ Microbiol **74:** 3718–3729.

11. Finneran KT, Housewright ME, Lovley DR. 2002. Multiple influences of nitrate on uranium solubility during bioremediation of uranium-contaminated subsurface sediments. Environ Microbiol **4:** 510–516.

12. Moon HS, Komlos J, Jaffe PR. 2007. Uranium reoxidation in previously bioreduced sediment by dissolved oxygen and nitrate. Environ Sci Technol **41:** 4587–4592.

13. Moon HS, Komlos J, Jaffe PR. 2009. Biogenic U(IV) oxidation by dissolved oxygen and nitrate in sediment after prolonged U(VI)/Fe(III)/SO_4^{2-} reduction. J Contam Hydrol **105:** 18–27.

14. Barberan A, Bates ST, Casamayor EO, Fierer N. 2012. Using network analysis to explore co-occurrence patterns in soil microbial communities. ISME J **6:** 343–351.

15. Chow CE, Sachdeva R, Cram JA, Steele JA, Needham DM, Patel A, Parada AE, Fuhrman JA. 2013. Temporal variability and coherence of euphotic zone bacterial communities over a decade in the Southern California Bight. ISME J **7:** 2259–2273.

16. Ju F, Zhang T. 2014. Bacterial assembly and temporal dynamics in activated sludge of a full-scale municipal wastewater treatment plant. ISME J 8(9) 1–13.

17. Luo J, Wu WM, Carley J, Ruan C, Gu B, Jardine PM, Criddle CS, Kitanidis PK. 2007. Hydraulic performance analysis of a multiple injection-extraction well system. J Hydrol **336**: 294–302.

18. W**u WM, Carley J, Gentry T, Ginder-Vogel MA, Fienen M, Mehlhorn T, Yan H, Caroll S,**

Pace MN, Nyman J, Luo J, Gentile ME, Fields MW, Hickey RF, Gu BH, Watson D, Cirpka OA, Zhou JZ, Fendorf S, Kitanidis PK, Jardine PM, Criddle CS. 2006b. Pilot-scale in situ bioremediation of uranium in a highly contaminated aquifer. 2: U(VI) reduction and geochemical control of U(VI) bioavailability. Environ Sci Technol **40**:3986–3995.

19. Wu WM, Watson DB, Luo J, Carley J, Mehlhorn T, Kitanidis PK, Jardine PM, Criddle CS. 2013. Surge block method for controlling well clogging and sampling sediment during bioremediation. Water Res 47 (17): 6566–6573.

20. Claesson MJ, Wang QO, O'Sullivan O, Greene-Diniz R, Cole JR, Ross RP, O'Toole PW. 2010. Comparison of two next-generation sequencing technologies for resolving highly complex microbiota composition using tandem variable 16S rRNA gene regions. Nucleic Acids Res **38**.

21. Caporaso JG, Kuczynski J, Stombaugh J, Bittinger K, Bushman FD, Costello EK, Fierer N, Peña AG, Goodrich JK, Gordon JI, Huttley GA, Kelley ST, Knights D, Koenig JE, Ley RE, Lozupone CA, McDonald D, Muegge BD, Pirrung M, Reeder J, Sevinsky JR, Turnbaugh PJ, Walters WA, Widmann J, Yatsunenko T, Zaneveld J, Knight R. 2010. QIIME allows analysis of high-throughput community sequencing data. Nat Methods **7:** 335–336.

22. Reeder J, Knight R. 2010. Rapidly denoising pyrosequencing amplicon reads by exploiting rank-abundance distributions. Nat Methods **7:** 668–669.

23. Quince C, Lanzen A, Davenport RJ, Turnbaugh PJ. 2011. Removing noise From pyrosequenced amplicons. BMC Bioinformatics **12**.

24. Edgar RC. 2010. Search and clustering orders of magnitude faster than BLAST. Bioinformatics **26:** 2460–2461.

25. Wang Q, Garrity GM, Tiedje JM, Cole JR. 2007. Naive Bayesian classifier for rapid assignment of rRNA sequences into the new bacterial taxonomy. Appl Environ Microbiol **73:** 5261–5267.

26. Hammer Ø, Harper DAT, Ryan PD. 2001. PAST: Paleontological statistics software package for education and data analysis. Palaeontologia Electronica 4(1):1–9

27. R Development Core Team. 2011. R: A language and environment for statistical computing. R Foundation for Statistical Computing: Vienna, Austria. ISBN 3-900051-07-0, available at http://www.R-project.org/.

28. Dufrene M, Legendre P. 1997. Species assemblages and indicator species: the need for a flexible asymmetrical approach. Ecol Monogr **67:** 345–366.

29. Oksanen J, Kindt R, Legendre P, O'Hara B, Simpson GL, Solymos P.2007. Vegan: community ecology package. *R package version1:8*.

30. Csárdi G, Nepusz T. 2006. The igraph software package for complex network research. Inter J Complex Syst **1695**.

31. Harrell J, Frank E. 2008. Hmisc: harrell miscellaneous. *R package version 35-2*.

32. Bastian M, Heymann S, Jacomy M. 2009. Gephi: an open source software for exploring and manipulating networks. Proceedings of the Third International ICWSM Conference (ICWSM) **8:**

361–362.

33. Watson, DB., Wu WM, Mehlhorn T, Tang G, Earles J, Lowe K, Gihring TM, Zhang G, Phillips J, Boyanov MI, Spalding BP, Schadt CW, Kemner KM, Criddle CS, Jardine PM, Brooks SC. 2013. In situ bioremediation of uranium with emulsified vegetable oil as the electron donor. Environ Sci Technol. **47** : 6440–6448.

34. Kuang JL, Huang LN, Chen LX, Hua ZS, Li SJ, Hu M, Li JT, Shu WS. 2013. Contemporary environmental variation determines microbial diversity patterns in acid mine drainage. ISME J **7:** 1038–1050.

35. Lin XJ, McKinley J, Resch CT, Kaluzny R, Lauber CL, Fredrickson J, Knight R, Konopka A.2012. Spatial and temporal dynamics of the microbial community in the Hanford unconfined aquifer. ISME J **6:** 1665–1676.

36. Fagervold SK, Bourgeois S, Pruski AM, Charles F, Kerhervé P, Vétion G, Galand PE. 2014. River organic matter shapes microbial communities in the sediment of the Rhône prodelta. ISME J 8:2327–2338

37. Reith F, Brugger J, Zammit CM, Gregg AL, Goldfarb KC, Andersen GL, DeSantis TZ, Piceno YM, Brodie EL, Lu ZM, He ZL, Zhou JZ, Wakelin SA. 2012. Influence of geogenic factors on microbial communities in metallogenic Australian soils. ISME J **6:** 2107–2118.

38. Van Nostrand JD, Wu WM, Wu LY, Deng Y, Carley J, Carroll S, He ZL, Gu BH, Luo J, Criddle CS, Watson DB, Jardine PM, Marsh TL, Tiedje JM, Hazen TC, Zhou JZ. 2009.

GeoChip-based analysis of functional microbial communities during the reoxidation of a bioreduced uranium-contaminated aquifer. Environ Microbiol **11:** 2611–2626.

39. Du X, Boonchayaanant B, Wu WM, Fendorf S, Bargar J, Criddle C. 2011. Reduction of uranium (VI) by soluble iron(II) conforms with thermodynamic predictions. Environ Sci Technol **45 (11):** 4718–4725.

40. O'Loughlin EJ, Kelly SD, Cook RE, Csencsits R, Kemner KM. 2003. Reduction of uranium(VI) by mixed iron(II/iron(III) hydroxide (green rust): Formation of UO(2) manoparticies. Environ Sci Technol **37:** 721–727.

41. Brodie EL, DeSantis TZ, Joyner DC, Baek SM, Larsen JT, Andersen GL, Hazen TC, Richardson PM, Herman DJ, Tokunaga TK, Wan JM, Firestone MK. 2006. Application of a high-density oligonucleotide microarray approach to study bacterial population dynamics during uranium reduction and reoxidation. Appl Environ Microbiol **72:** 6288–6298.

42. Wan JM, Tokunaga TK, Brodie E, Wang ZM, Zheng ZP, Herman D, Hazen TC , Firestone MK , Sutton SR. 2005. Reoxidation of bioreduced uranium under reducing conditions. Environ Sci Technol **39:** 6162–6169.

43. Chao A, Chazdon RL, Colwell RK, Shen TJ. 2006. Abundance-based similarity indices and their estimation when there are unseen species in samples. Biometrics **62:** 361–371.

44. Coates JD, Ellis DJ, Gaw CV, Lovley DR. 1999. Geothrix fermentans gen. nov., sp nov., a novel Fe(III)-reducing bacterium from a hydrocarbon-contaminated aquifer. Int J Syst Bacteriol **49:**

1615–1622.

45. Nevin KP, Lovley DR. 2000. Potential for nonenzymatic reduction of Fe(III) via electron shuttling in subsurface sediments. Environ Sci Technol **34:** 2472–2478.

46. Bier RL, Voss KA, Bernhardt ES. 2014. Bacterial community responses to a gradient of alkaline mountaintop mine drainage in Central Appalachian streams. ISME J 8(12):1–13.

47. Seitz, HJ, Cypionka, H. 1986. Chemolithotrophic growth of *Desulfovibrio desulfuricans* with hydrogen coupled to ammonification of nitrate or nitrite. Arch. Microbiol. **146**: 63-67.

48. Tiedje, J M. 1988. Ecology of denitrification and dissimilatory nitrate reduction to ammonium. In *Biology of Anaerobic Microorganisms;* Zhender, A. J. B., Ed.; John Wiley & Sons: New York, pp 179-244.

49. Weber, K A, Urrutia, M M, Churchill, PF, Kukkadapu, RK, Roden, EE. 2006. Anaerobic redox cycling of ion by freshwater sediment microorganisms. *Environ. Microbiol.* **8**: 100-113.

50. Spain AM, Peacock AD, Istok JD, Elshahed MS, Najar FZ, Roe BA, White DC, Krumholz LR. 2007. Identification and isolation of a Castellaniella species important during biostimulation of an acidic nitrate- and uranium-contaminated aquifer. Appl Environ Microbiol **73:** 4892–4904.

51. Akob DM, Mills HJ, Gihring TM, Kerkhof L, Stucki JW, Anastácio AS, Chin KJ, Küsel K, Palumbo AV, Watson DB, Kostka JE. 2008. Functional diversity and electron donor dependence of microbial populations capable of U(VI) reduction in radionuclide-contaminated subsurface sediments. Appl Environ Microbiol **74:** 3159–3170.

52. Hemme CL, Deng Y, Gentry TJ, Fields MW, Wu LY, Barua S, Barry K, Tringe SG, Watson DB, He ZL, Hazen TC, Tiedje JM, Rubin EM, Zhou JZ. 2010. Metagenomic insights into evolution of a heavy metal-contaminated groundwater microbial community. ISME J **4:** 660–672.

53. Van Den Heuvel RN, Der Biezen EV, Jetten MSM, Hefting MM, Kartal B. 2010 .Denitrification at pH 4 by a soil-derived Rhodanobacter-dominated community. Environ Microbiol 12(12): 3264-3271

54. Auguet O, Pijuan M, Guasch-Balcells H, Borrego CM, Gutierrez O. 2015. Implications of downstream nitrate dosage in anaerobic sewers to control sulfide and methane emissions. Water Res **68:** 522–532.

55. Podosokorskaya OA, Kadnikov VV, Gavrilov SN, Mardanov AV, Merkel AY, Karnachuk OV, Ravin NV, Bonch-Osmolovskaya EA, Kublanov IV. 2013. Characterization of Melioribacter roseus gen. nov., sp nov., a novel facultatively anaerobic thermophilic cellulolytic bacterium from the class Ignavibacteria, and a proposal of a novel bacterial phylum Ignavibacteriae. Environ Microbiol **15:** 1759–1771.

56. Junker B, Schreiber F. 2008. Correlation Networks. *Analysis of biological networks*. Wiley-Interscience.

57. Horner-Devine MC, Silver JM, Leibold MA, Bohannan BJM, Colwell RK, Fuhrman JA, Green JL, Kuske CR, Martiny JB, Muyzer G, Ovreås L, Reysenbach AL, Smith VH. 2007. A comparison of taxon co-occurrence patterns for macro- and microorganisms. Ecol **88:** 1345–1353.

58. Achtman M, Wagner M. 2008. Microbial diversity and the genetic nature of microbial species.

Nat Rev Microbiol **6:** 431–440.

Figure Legends

Figure 1. NMDS plot showing the microbial community differences (at genus level) for all the selected wells before and after the long-term invasion of groundwater. Samples marked in black and in blue represent samples collected from the bioreduction and reoxidation stages, respectively. Solid circles represent inactive wells and empty circles represent active wells classified according to the bromide recovery ratios during the bioreduction stage.

Figure 2. (a) Abundance of different phyla in all the sediment samples during the bioreduction and reoxidation stages. Samples collected from the bioactive wells of FW101-2, FW101-3, FW102-2, FW102-3, FW104, and FW026 during the bioreduction and reoxidation stages are boxed with blue and green rectangles, respectively. (b) *Firmicutes* composition in sample of FW101-2-O. The numbers after the taxonomic ranks are the abundance ratios of the corresponding taxon in phylum of *Firmicutes* and sample of FW101-2-O, respectively.

Figure 3. Abundance of the 77 major (>0.5% in at least one sample) genera in the 30 sediment samples before and after the long-term groundwater invasion. Major genera with occupancies of >80% and average abundance of >0.1% were defined as common genera and are in bold font. The genera marked with blue triangles are U(VI)-reducing bacteria.

Figure 4. A canonical correspondence analysis plot reveals the relationships between the target microbial genera and the geochemical parameters. Three U(VI)-reducing genera, *Geobacter, Desulfovibrio,* and *Ferribacterium* (in bold font), are also indicator genera at the bioreduction stage.

Figure 5. The network analysis revealing the co-occurrence patterns among microbial taxa and environmental parameters. (a) The nodes are colored according to modularity class. (b) The nodes are colored according to functional taxa and environmental parameters. A connection represents a strongly (Spearman's correlation coefficient ρ >0.6) and significantly positive correlation (P-value <0.01). The size of each node is proportional to the number of connections, i.e., the degree. Three U(VI)-reducing genera, *Geobacter*, *Desulfovibrio,* and *Ferribacterium* (in bold font), are also indicator genera at the bioreduction stage.

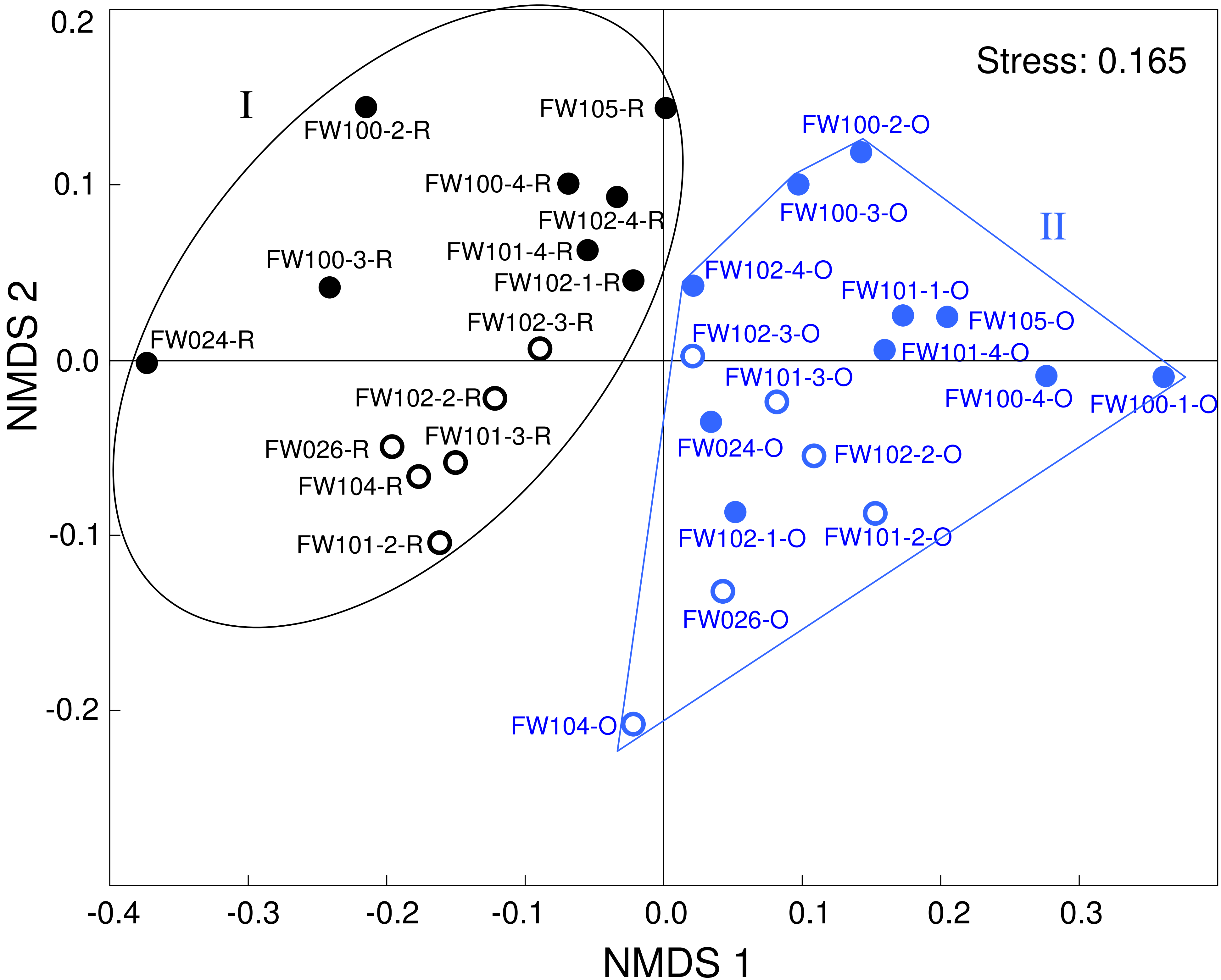
Stress: 0.165
I
II
FW105-R
FW100-2-R
FW100-4-R
FW102-4-R
FW101-4-R
FW100-3-R
FW102-1-R
FW102-3-R
FW024-R
FW102-2-R
FW026-R
FW101-3-R
FW104-R
FW101-2-R
FW100-2-O
FW100-3-O
FW102-4-O
FW101-1-O
FW105-O
FW102-3-O
FW101-4-O
FW101-3-O
FW100-4-O
FW100-1-O
FW024-O
FW102-2-O
FW102-1-O
FW101-2-O
FW026-O
FW104-O
NMDS 1
NMDS 2
0.2
0.1
0.0
-0.1
-0.2
-0.4
-0.3
-0.2
-0.1
0.0
0.1
0.2
0.3

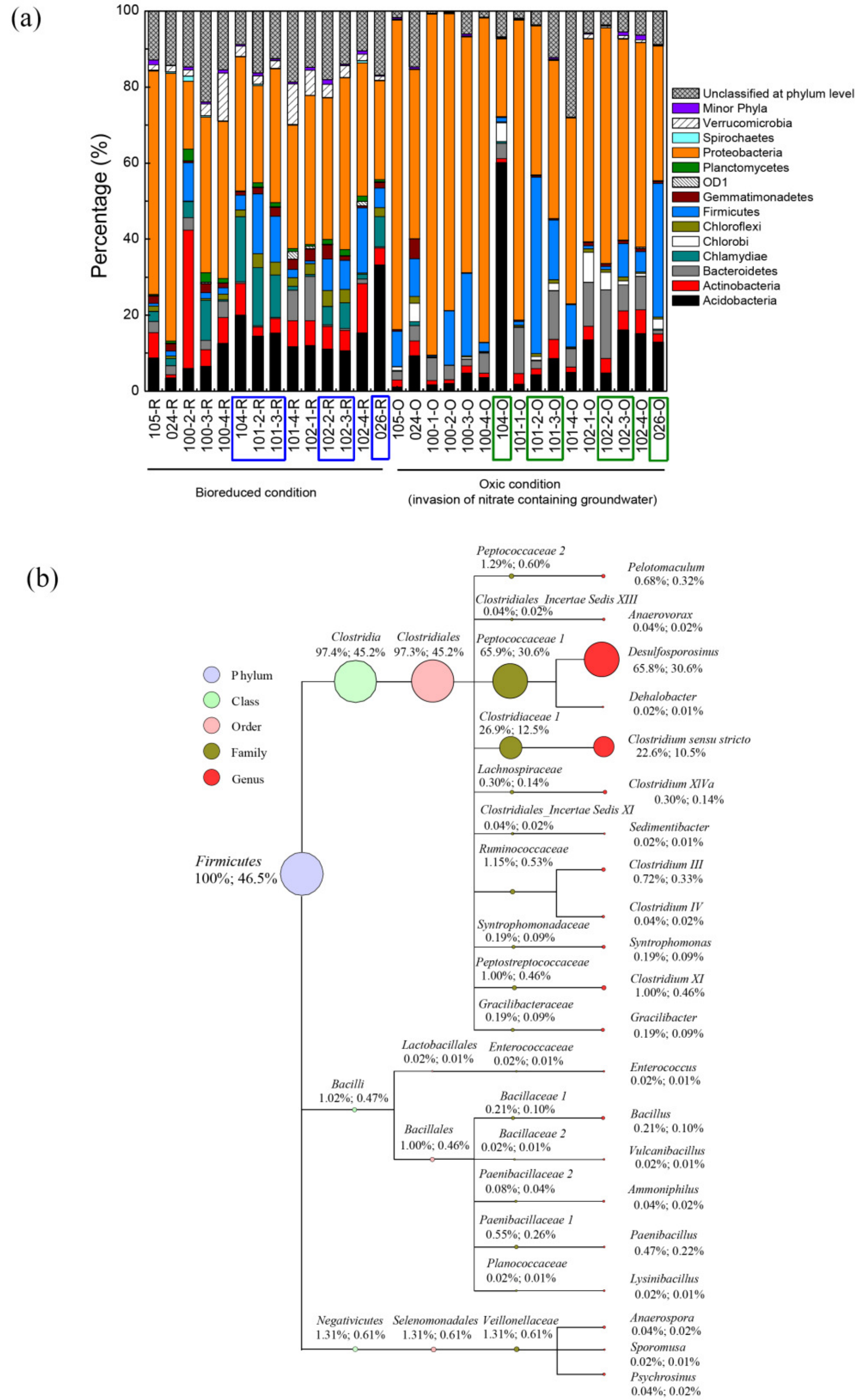
(a)
Percentage (%)
100
80
60
40
20
0
Unclassified at phylum level
Minor Phyla
Verrucomicrobia
Spirochaetes
Proteobacteria
Planctomycetes
OD1
Gemmatimonadetes
Firmicutes
Chloroflexi
Chlorobi
Chlamydiae
Bacteroidetes
Actinobacteria
Acidobacteria
105-R
024-R
100-2-R
100-3-R
100-4-R
104-R
101-2-R
101-3-R
101-4-R
102-1-R
102-2-R
102-3-R
102-4-R
026-R
105-O
024-O
100-1-O
100-2-O
100-3-O
100-4-O
104-O
101-1-O
101-2-O
101-3-O
101-4-O
102-1-O
102-2-O
102-3-O
102-4-O
026-O
Bioreduced condition
Oxic condition
(invasion of nitrate containing groundwater)
(b)
Phylum
Class
Order
Family
Genus
Firmicutes
100%; 46.5%
Clostridia
97.4%; 45.2%
Clostridiales
97.3%; 45.2%
Peptococcaceae 2
1.29%; 0.60%
Pelotomaculum
0.68%; 0.32%
Clostridiales_Incertae Sedis XIII
0.04%; 0.02%
Anaerovorax
0.04%; 0.02%
Peptococcaceae 1
65.9%; 30.6%
Desulfosporosinus
65.8%; 30.6%
Dehalobacter
0.02%; 0.01%
Clostridiaceae 1
26.9%; 12.5%
Clostridium sensu stricto
22.6%; 10.5%
Lachnospiraceae
0.30%; 0.14%
Clostridium XlVa
0.30%; 0.14%
Clostridiales_Incertae Sedis XI
0.04%; 0.02%
Sedimentibacter
0.02%; 0.01%
Ruminococcaceae
1.15%; 0.53%
Clostridium III
0.72%; 0.33%
Clostridium IV
0.04%; 0.02%
Syntrophomonadaceae
0.19%; 0.09%
Syntrophomonas
0.19%; 0.09%
Peptostreptococcaceae
1.00%; 0.46%
Clostridium XI
1.00%; 0.46%
Gracilibacteraceae
0.19%; 0.09%
Gracilibacter
0.19%; 0.09%
Bacilli
1.02%; 0.47%
Lactobacillales
0.02%; 0.01%
Enterococcaceae
0.02%; 0.01%
Enterococcus
0.02%; 0.01%
Bacillales
1.00%; 0.46%
Bacillaceae 1
0.21%; 0.10%
Bacillus
0.21%; 0.10%
Bacillaceae 2
0.02%; 0.01%
Vulcanibacillus
0.02%; 0.01%
Paenibacillaceae 2
0.08%; 0.04%
Ammoniphilus
0.04%; 0.02%
Paenibacillaceae 1
0.55%; 0.26%
Paenibacillus
0.47%; 0.22%
Planococcaceae
0.02%; 0.01%
Lysinibacillus
0.02%; 0.01%
Negativicutes
1.31%; 0.61%
Selenomonadales
1.31%; 0.61%
Veillonellaceae
1.31%; 0.61%
Anaerospora
0.04%; 0.02%
Sporomusa
0.02%; 0.01%
Psychrosinus
0.04%; 0.02%

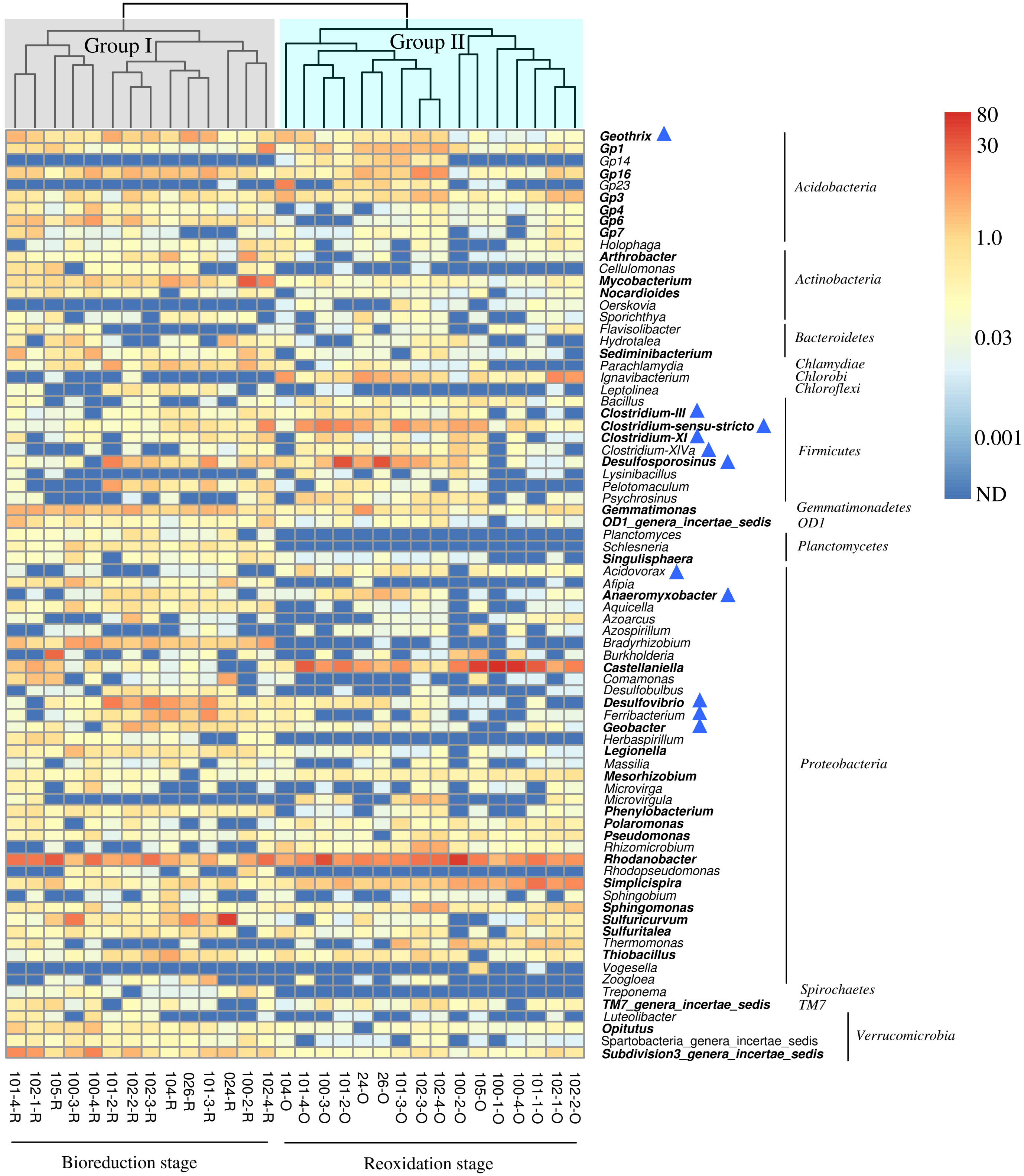

Group I
Group II
Geothrix
Gp1
Gp14
Gp16
Gp23
Gp3
Gp4
Gp6
Gp7
Holophaga
Arthrobacter
Cellulomonas
Mycobacterium
Nocardioides
Oerskovia
Sporichthya
Flavisolibacter
Hydrotalea
Sediminibacterium
Parachlamydia
Ignavibacterium
Leptolinea
Bacillus
Clostridium-III
Clostridium-sensu-stricto
Clostridium-XI
Clostridium-XIVa
Desulfosporosinus
Lysinibacillus
Pelotomaculum
Psychrosinus
Gemmatimonas
OD1_genera_incertae_sedis
Planctomyces
Schlesneria
Singulisphaera
Acidovorax
Afipia
Anaeromyxobacter
Aquicella
Azoarcus
Azospirillum
Bradyrhizobium
Burkholderia
Castellaniella
Comamonas
Desulfobulbus
Desulfovibrio
Ferribacterium
Geobacter
Herbaspirillum
Legionella
Massilia
Mesorhizobium
Microvirga
Microvirgula
Phenylobacterium
Polaromonas
Pseudomonas
Rhizomicrobium
Rhodanobacter
Rhodopseudomonas
Simplicispira
Sphingobium
Sphingomonas
Sulfuricurvum
Sulfuritalea
Thermomonas
Thiobacillus
Vogesella
Zoogloea
Treponema
TM7_genera_incertae_sedis
Luteolibacter
Opitutus
Spartobacteria_genera_incertae_sedis
Subdivision3_genera_incertae_sedis
Acidobacteria
Actinobacteria
Bacteroidetes
Chlamydiae
Chlorobi
Chloroflexi
Firmicutes
Gemmatimonadetes
OD1
Planctomycetes
Proteobacteria
Spirochaetes
TM7
Verrucomicrobia
80
30
1.0
0.03
0.001
ND
101-4-R
102-1-R
105-R
100-3-R
100-4-R
101-2-R
102-2-R
102-3-R
104-R
026-R
101-3-R
024-R
100-2-R
102-4-R
104-O
101-4-O
100-3-O
101-2-O
24-O
26-O
101-3-O
102-3-O
102-4-O
100-2-O
105-O
100-1-O
100-4-O
101-1-O
102-1-O
102-2-O
Bioreduction stage
Reoxidation stage

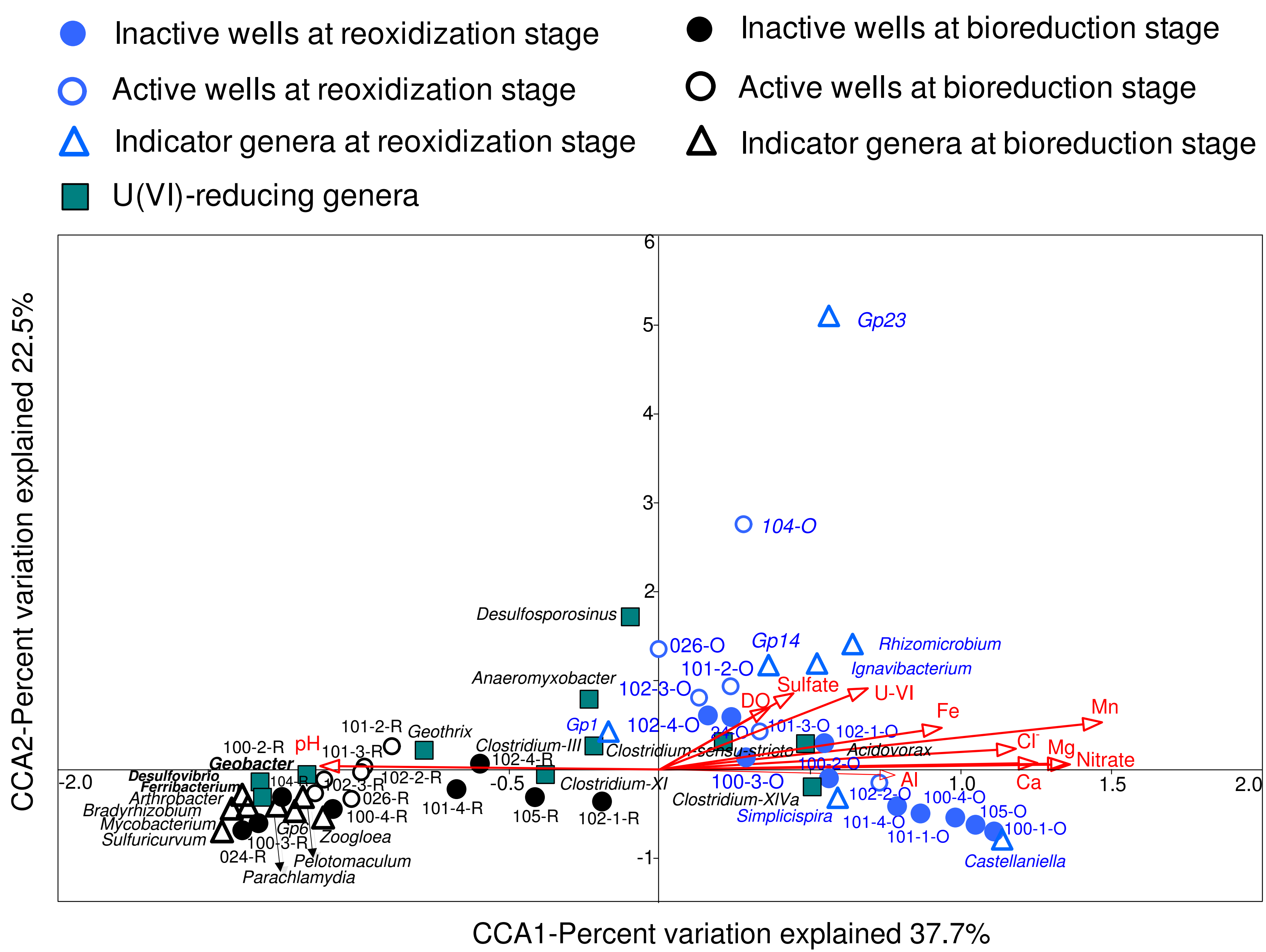

Inactive wells at reoxidization stage
Active wells at reoxidization stage
Indicator genera at reoxidization stage
U(VI)-reducing genera
Inactive wells at bioreduction stage
Active wells at bioreduction stage
Indicator genera at bioreduction stage
CCA2-Percent variation explained 22.5%
CCA1-Percent variation explained 37.7%
Gp23
104-O
Desulfosporosinus
026-O
Gp14
Rhizomicrobium
101-2-O
Ignavibacterium
Anaeromyxobacter
102-3-O
Sulfate
U-VI
DO
Fe
Mn
Gp1
102-4-O
101-3-O
102-1-O
Cl-
Mg
Nitrate
Geothrix
Clostridium-III
Clostridium sensu stricto
Acidovorax
100-2-O
Al
Ca
101-2-R
100-2-R
pH
101-3-R
102-4-R
Geobacter
Desulfovibrio
Ferribacterium
Arthrobacter
Bradyrhizobium
Mycobacterium
Sulfuricurvum
104-R
102-3-R
102-2-R
026-R
100-4-R
101-4-R
105-R
102-1-R
Clostridium-XI
100-3-O
Clostridium-XIVa
Simplicispira
102-2-O
100-4-O
105-O
101-4-O
101-1-O
100-1-O
Castellaniella
Gp6
Zoogloea
100-3-R
024-R
Pelotomaculum
Parachlamydia

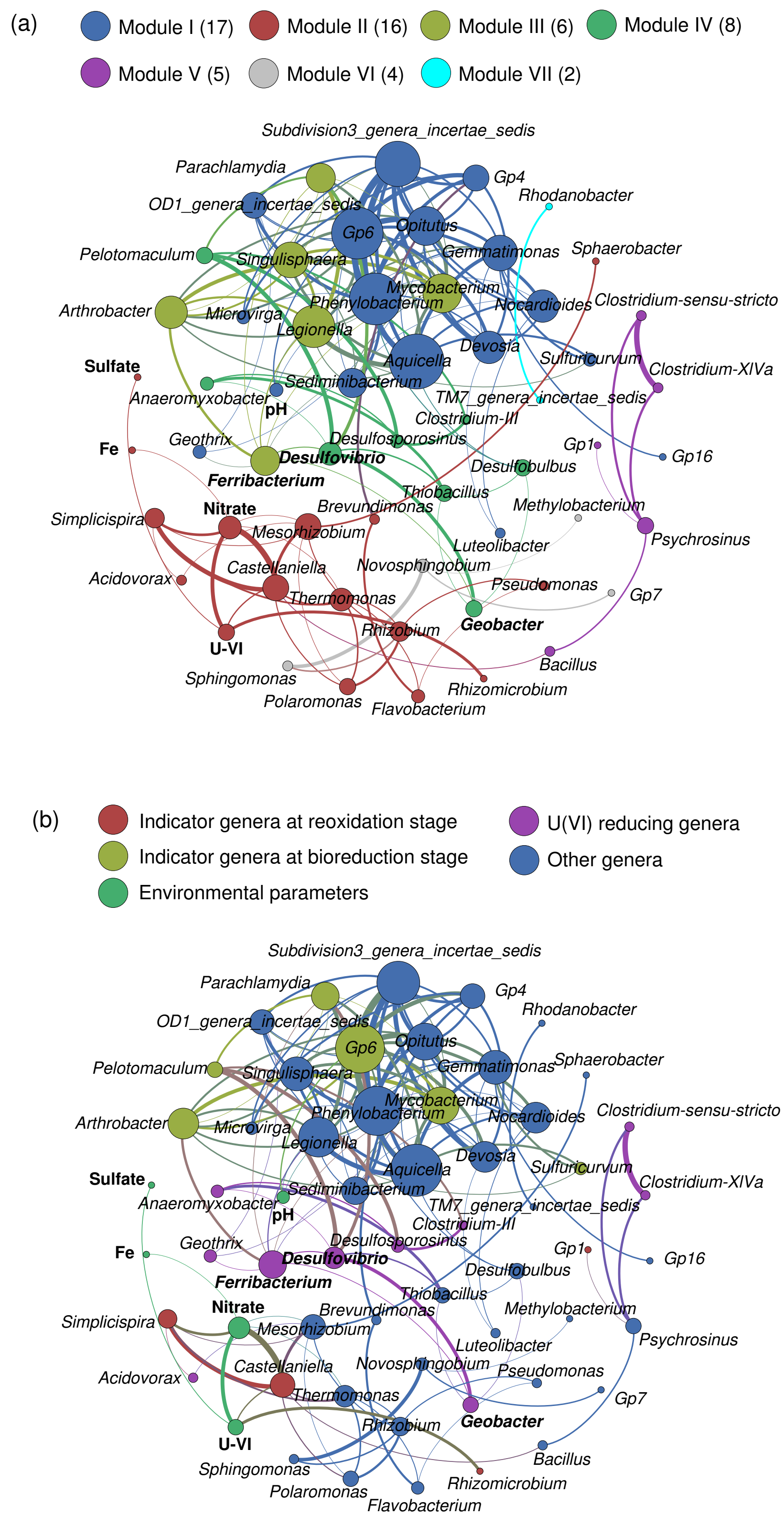
(a)
Module I (17)
Module II (16)
Module III (6)
Module IV (8)
Module V (5)
Module VI (4)
Module VII (2)
Subdivision3_genera_incertae_sedis
Parachlamydia
Gp4
Rhodanobacter
OD1_genera_incertae_sedis
Gp6
Opitutus
Pelotomaculum
Singulisphaera
Gemmatimonas
Sphaerobacter
Mycobacterium
Arthrobacter
Microvirga
Phenylobacterium
Nocardioides
Clostridium-sensu-stricto
Legionella
Sulfate
Devosia
Aquicella
Sulfuricurvum
Clostridium-XIVa
Sediminibacterium
Anaeromyxobacter
pH
TM7_genera_incertae_sedis
Clostridium-III
Fe
Geothrix
Desulfosporosinus
Gp1
Gp16
Desulfovibrio
Desulfobulbus
Ferribacterium
Thiobacillus
Nitrate
Brevundimonas
Methylobacterium
Simplicispira
Mesorhizobium
Psychrosinus
Luteolibacter
Castellaniella
Novosphingobium
Acidovorax
Pseudomonas
Gp7
Thermomonas
Geobacter
Rhizobium
U-VI
Bacillus
Sphingomonas
Rhizomicrobium
Polaromonas
Flavobacterium
(b)
Indicator genera at reoxidation stage
Indicator genera at bioreduction stage
Environmental parameters
U(VI) reducing genera
Other genera
Subdivision3_genera_incertae_sedis
Parachlamydia
Gp4
Rhodanobacter
OD1_genera_incertae_sedis
Gp6
Opitutus
Pelotomaculum
Gemmatimonas
Sphaerobacter
Singulisphaera
Mycobacterium
Phenylobacterium
Arthrobacter
Nocardioides
Clostridium-sensu-stricto
Microvirga
Legionella
Devosia
Sulfuricurvum
Aquicella
Sulfate
Clostridium-XIVa
Sediminibacterium
Anaeromyxobacter
TM7_genera_incertae_sedis
pH
Clostridium-III
Desulfosporosinus
Fe
Geothrix
Gp1
Desulfovibrio
Gp16
Desulfobulbus
Ferribacterium
Thiobacillus
Nitrate
Brevundimonas
Methylobacterium
Simplicispira
Mesorhizobium
Psychrosinus
Luteolibacter
Castellaniella
Novosphingobium
Pseudomonas
Acidovorax
Thermomonas
Gp7
Rhizobium
Geobacter
U-VI
Bacillus
Sphingomonas
Rhizomicrobium
Polaromonas
Flavobacterium

Table 1. Geochemical characteristics of groundwater in the subsurface of the test site during the bioreduction stage (October 2005) and the reoxidation stage (October 2012)

Well	Status	Groundwater														Sediment	
		pH	ORP (mV)	DO (mg/L)	Sulfate (mM)	Nitrate (mM)	S^{2-} (mM)	NH_4^+ (mM)	Cl^- (mM)	U-VI (μM)	Al (mM	Ca (mM)	Mg (mM)	Fe (mM)	Mn (mM)	U (mg/kg)	Fe (g/kg)
FW024	R, A	5.87	NA	0.06	1.58	0.011	0.005	NA	2.31	0.092	0.013	0.792	0.45	0.003	0.014	0.37	50.80
	O	4.81	340	0.33	2.48	166.8	0.00	NA	8.04	12.67	2.77	51.2	11.7	0.057	2.82	0.97	33.35
FW026	R, A	5.74	NA	0.08	1.20	0.007	0.04	NA	2.36	0.525	0.02	0.64	0.32	0.006	0.071	5.92	47.10
	O	6.52	288	3.45	1.07	10.14	0.00	NA	1.59	0.949	0.018	3.12	0.88	0.003	0.29	1.73	28.68
FW100-1	O	5.76	277	0.37	2.03	238.6	0.00	NA	9.84	5.999	0.31	81.8	16.81	0.095	3.26	0.22	44.90
FW100-2	R	5.50	NA	0.08	1.54	0.017	0.00	NA	2.38	0.979	0.018	0.776	0.325	0.003	0.046	0.98	55.60
	O	3.54	321	0.16	5.83	142.1	0.00	0.421	6.36	90.60	10.53	33.3	10.10	0.054	2.76	1.19	26.65
FW100-3	R	5.87	NA	0.08	1.45	0.023	0.00	NA	2.27	0.326	0.014	0.775	0.432	0.003	0.026	1.10	32.40
	O	4.16	299	0.24	2.76	61.24	0.00	0.232	3.77	20.61	2.04	18.34	5.10	0.033	1.42	1.44	24.22
FW100-4	R	5.80	NA	0.06	1.44	1.597	0.00	NA	2.26	1.505	0.093	1.60	0.47	0.003	0.082	1.50	36.20
	O	4.01	296	0.11	1.23	52.15	0.00	NA	2.55	14.86	3.04	12.12	5.74	0.015	0.72	1.26	30.77
FW101-1	O	5.36	236	0.36	0.15	396.4	0.00	NA	11.4	1.838	0.019	149.9	34.47	0.164	3.42	0.05	34.40
FW101-2	R, A	6.23	NA	0.06	1.07	0.000	0.43	<0.01[a]	2.32	0.150	0.00	0.67	0.30	0.034	0.073	1.25	28.59
	O	4.80	213	0.24	3.09	100.2	0.00	0.193	5.56	32.16	2.20	32.3	8.45	0.195	2.52	2.18	28.24
FW101-3	R, A	6.10	NA	0.05	1.20	0.003	0.36	<0.01[a]	2.31	0.111	0.01	0.62	0.31	0.005	0.063	1.52	25.51
	O	4.41	276	0.18	2.01	57.99	0.00	0.194	3.92	8.790	1.19	18.95	5.41	0.036	1.32	1.07	25.36
FW101-4	R	5.56	NA	0.05	1.41	0.290	0.00	NA	2.485	0.634	0.103	0.695	0.282	0.005	0.047	0.62	29.40
	O	4.39	118	0.25	1.06	44.57	0.00	NA	2.96	2.576	1.91	12.36	5.45	0.015	0.56	0.79	30.43
FW102-1	R	6.38	NA	0.07	0.29	34.40	0.00	NA	2.65	0.739	0.016	13.15	2.824	0.014	0.56	0.04	42.60
	O	5.56	216	0.23	0.17	146.5	0.00	NA	6.14	1.351	0.009	54.9	11.8	0.057	1.40	0.03	31.08
FW102-2	R, A	6.45	NA	0.06	1.01	0.011	0.16	<0.01[a]	2.32	0.083	0.01	0.80	0.31	0.039	0.077	0.52	29.23
	O	5.55	57	0.14	0.98	57.73	0.00	0.083	3.92	1.475	0.165	21.4	5.18	0.025	1.13	0.15	28.44
FW102-3	R, A	6.23	NA	0.06	1.10	0.001	0.11	<0.01[a]	3.91	0.061	0.01	0.62	0.31	0.045	0.082	0.88	32.25
	O	4.93	163	0.22	1.49	27.00	0.00	0.157	2.50	7.509	0.30	7.09	2.84	0.049	0.92	1.81	32.89
FW102-4	R	4.43	-100	0.06	1.23	0.018	0.00	NA	2.44	5.427	0.103	0.285	0.206	0.002	0.036	0.48	36.40
	O	4.66	177	0.23	1.38	16.86	0.00	NA	1.85	7.875	0.30	4.09	2.00	0.029	0.66	1.33	32.89
FW104	R, A	5.75	NA	0.09	1.18	0.000	0.30	NA	2.34	0.569	0.02	0.65	0.32	0.031	0.070	10.30	199.10
	O	5.52	145	0.17	4.81	130.8	0.00	NA	7.30	67.01	0.075	50.3	11.37	0.071	2.63	NA	NA
FW 105	R	4.66	200	0.09	1.73	2.108	0.00	NA	2.11	5.239	0.187	1.145	0.345	0.000	0.09	0.98	30.42
	O	4.40	304	0.52	2.16	134.6	0.00	0.213	4.83	8.865	1.57	41.7	9.94	0.045	1.54	1.94	20.55

O: reoxidation stage; R: bioreduction stage; A: previously bioactive site; NA: not analyzed; [a]: lower than the detection limit; The well system is described in Figure S1.

Table 2. SIMPER analysis of bacterial community dissimilarity during bioreduction and after groundwater invasion

Taxon	Mean abundance %		Average dissimilarity	Contribution %	Cumulative %
	Bioreduction stage	Reoxidation stage			
Castellaniella	0.51	17.8	13.9	17.7	17.7
Rhodanobacter	8.26	12.6	8.54	10.9	28.7
Desulfosporosinus	1.61	4.92	4.55	5.81	34.5
Sulfuricurvum	5.07	0.12	4.17	5.34	39.8
Clostridium-sensu-stricto	0.77	3.13	2.70	3.45	43.3
Mycobacterium	3.25	0.12	2.69	3.45	46.7
Simplicispira	0.51	3.32	2.53	3.23	49.9
Desulfovibrio	2.71	0.17	2.44	3.12	53.1
Ignavibacterium	0.004	1.98	1.96	2.51	55.6
Subdivision3_genera_incertae_sedis	2.30	0.23	1.81	2.32	57.9
Bradyrhizobium	1.93	0.002	1.69	2.16	60.0
Gemmatimonas	1.81	0.69	1.41	1.80	61.8
Gp16	1.41	1.35	1.40	1.79	63.6
Burkholderia	1.27	0.35	1.24	1.59	65.2
Gp1	0.84	1.01	1.17	1.50	66.7
Geothrix	1.38	0.43	1.11	1.43	68.1
Ferribacterium	1.23	0.05	1.10	1.41	69.5
Gp6	1.20	0.05	1.00	1.28	70.8
Gp23	0.001	0.84	0.89	1.14	72.0
Parachlamydia	1.01	0.07	0.87	1.11	73.1

Table 3. Indicator genera of the bioactive wells during bioreduction and after long-term reoxidation

Cluster in Fig. S8	Indicator genera	Cluster affiliation	Indicator value [a]	*P* value [b]	Average relative abundance (%) [c]	
					Bioreduction stage	Reoxidation stage
I	*Castellaniella*	Reoxidation stage	0.985	0.01	0.08	5.30
	Ignavibacterium		0.997	0.01	0.01	2.69
	Simplicispira		0.843	0.02	0.48	2.55
	Gp23		0.833	0.03	0.00	2.09
	Gp1		0.944	0.03	0.07	1.17
	Rhizomicrobium		0.981	0.01	0.02	0.80
	Gp14		0.833	0.03	0.00	0.59
II	***Desulfovibrio*** [d]	Bioreduction stage	0.955	0.02	6.10	0.29
	Ferribacterium [d]		0.961	0.01	2.58	0.10
	Sulfuricurvum		0.973	0.01	1.93	0.05
	Mycobacterium		0.926	0.01	1.55	0.12
	Bradyrhizobium		0.999	0.01	1.49	0.00
	Parachlamydia		0.943	0.01	1.49	0.09
	Pelotomaculum		0.938	0.01	1.49	0.10
	Geobacter [d]		0.880	0.02	1.22	0.17
	Gp6		0.938	0.01	0.69	0.05
	Arthrobacter		0.919	0.04	0.64	0.06
	Zoogloea		0.969	0.03	0.51	0.02

[a] The cutoff of the indicator value is 0.800.
[b] The cutoff of *P* value is 0.05 (1000-bootstrap test in indicator genera analysis). Only genera with indicator value >0.800 and *P* value <0.05 were considered as strong indicators.
[c] The cutoff of the indicator genera relative abundance is 0.5%
[d] The indicator genera marked with bold font are U(VI)-reducing genera
Note: Indicator values range from 0 to 1, with higher values for stronger indicators (Fortunato et al., 2013). Only genera with indicator value >0.800, P value <0.05 and average relative abundance >0.5% were considered good indicators.

Supplementary Material for

Bacterial Community Shift and Coexisting/Coexcluding Patterns Revealed by Network Analysis in A Bioreduced Uranium Contaminated Site after Reoxidation

Bing Li[1,2,3,4], Wei-Min Wu[2*], David B. Watson[3], Erick Cardenas[5], Yuanqing Chao[1,3], D. H. Phillips[6], Tonia Mehlhorn[3], Kenneth Lowe[3], Shelly D. Kelly[7], Pengsong Li[2,3,8], Huchun Tao[2,8], James M. Tiedje[5], Craig S. Criddle[2], Tong Zhang[1*]

[1] Department of Civil Engineering, The University of Hong Kong, Hong Kong, China
[2] Department of Civil and Environmental Engineering, William & Cloy Codiga Resource Recovery Research Center, Center for Sustainable Development and Global Competitiveness, Stanford University, Stanford, CA 94305-4020
[3] Environmental Sciences Division, Oak Ridge National Laboratory, P.O. Box 2008, Oak Ridge, Tennessee 37831
[4] Key Laboratory of Microorganism Application and Risk Control of Shenzhen, Graduate School at Shenzhen, Tsinghua University, China
[5] Center for Microbial Ecology, Michigan State University, East Lansing, Michigan 48824
[6] Queen's University of Belfast, Environmental Engineering Research Centre, School of Planning, Architecture and Civil Engineering, Belfast, Northern Ireland, UK.
[7] EXAFS Analysis, Bolingbrook, IL 60440, USA
[8]Peking University Shenzhen Graduate School, School of Environment and Energy, Key Laboratory for Heavy Metal Pollution Control and Reutilization, Shenzhen 518055, China

Tables

Table S1. Diversity comparison before and after long-term groundwater invasion

Table S2. Abundance shift of subdivision of *Proteobacteria* after long-term groundwater invasion

Table S3. Abundance shift of U(VI)-reducing genera between active wells and inactive wells

Table S4. Summary of canonical correspondence analysis results

Table S5. Co-occurring microbial genera of module hub

Table S6. The co-occurring genera shared by hubs of Module I and Module III

Table S7. The associations between environmental parameters and genera

Figures

Figure S1. Scheme of the well system in Area 3, Oak Ridge National Laboratory, DOE. Hydrology connectivity is shown with the spatial distributions of bromide recovery (as percentage, in color) and mean travel times (contour lines with units of hours).

Figure S2. NMDS plot showing the microbial community differences (at 3% cutoff-OTU level) for all the selected wells before and after the long-term invasion of groundwater. Pairwise community distances were determined using (a) weighted UniFrac algorithm (b) unweighted UniFrac algorithm. Black and blue colors represent the samples collected from the bioreduction and reoxidation stages, respectively. Solid circles represent inactive wells and empty circles represent active wells classified according to the bromide recovery ratios during the bioreduction stage.

Figure S3. NMDS plot showing the microbial community shift (at genus level) for all the selected wells before and after the long-term invasion of groundwater. Black and blue colors represent the samples collected from the bioreduction and reoxidation stages, respectively. Solid circles represent inactive wells and empty circles represent active wells classified according to the bromide recovery ratios during the bioreduction stage. The dashed lines with arrows indicate the coordinate position shift of each specific sample in the NDMS plot.

Figure S4. *Proteobacteria* composition at class level of samples during the bioreduction and reoxidation stages.

Figure S5. *Firmicutes* composition in sample of 101-2-R. The numbers after the taxonomic ranks are the abundance ratios of the corresponding taxons in the phylum of *Firmicutes* and sample of 101-2-R, respectively.

Figure S6. *Acidobacteria* composition in sample of 104-O. The numbers after the taxonomic ranks are the abundance ratios of the corresponding taxons in the phylum of *Acidobacteria* and sample of 104-O, respectively.

Figure S7. *Acidobacteria* composition in sample of 104-R. The numbers after the taxonomic ranks are the abundance ratios of the corresponding taxons in the phylum of *Acidobacteria* and 104-R, respectively.

Figure S8. Cluster analysis (CA) of bacterial profiles in active wells before and after the long-term invasion of groundwater. CA was conducted based on the Bray-Curtis distance calculated from the matrix of genus relative abundance using PAST software. Unweighted pair group mean average (UPGMA) was selected as the algorithm for CA.

Figure S9. Average relative abundance (y-axis) and occupancy (x-axis) of indicator genera at (a) bioreduction stage and (b) reoxidization stage. The genera located in the shaded area (gray color) belong to persistent genera with occupancies $\geqslant$80% (24 samples). The genera located in the shaded area (yellow color) belong to specialist genera with low occupancies $\leqslant$45% (13 samples).The genera marked with bold font are U(VI)-reducing genera.

Figure S10. The network analysis revealing the co-exclusion patterns among microbial taxa and environmental parameters. The nodes were colored according to functional taxa and environmental parameters. A connection represents a strongly (Spearman's correlation coefficient ρ<-0.6) and significantly (P-value <0.01) negative correlation. The size of each node is proportional to the number of connections, i.e., the degree. Three U(VI)-reducing genera, *Geobacter*, *Desulfovibrio,* and *Ferribacterium* (marked with bold font), are also indicator genera at the bioreduction stage.

S1 Network analysis

To visualize the correlations in the network interface, we constructed a correlation matrix by calculating all possible pairwise Spearman's rank correlations among the 63 genera (average abundance >0.1%) that occurred in at least 5 samples from the bioreduction stage and 6 samples from the reoxidation stage simultaneously, and 5 environmental variables (Steele et al., 2011). This preliminary filtering step removed the poorly represented genera that occurred in a limited number of samples and thus reduced the artificial association bias. A correlation between two items was considered statistically robust if the Spearman's correlation coefficient (ρ) was > 0.6 or $\rho < -0.6$ and the *P*-value was < 0.01 (Junker and Schreiber, 2008). To reduce the chances of obtaining false-positive results, the *P*-values were adjusted with a multiple testing correction using the Benjamini–Hochberg method (Benjamini and Hochberg 1995). The robust pairwise correlations of the genera and environmental parameters formed their co-occurrence networks.

S2 Bacterial community composition

As shown in Figure S4, *Proteobacteria* compositions at the class level of the samples during the bioreduction and reoxidation stages were further investigated to compare their abundance difference after the long-term groundwater invasion. For the bioactive wells, the subdivision of Alpha-, Beta-, Gamma-, and Delta-*Proteobacteria* was the dominant class at the bioreduction stage; while Alpha-, Beta-, and Gamma-*Proteobacteria* were the major class within *Proteobacteria* at the reoxidation stage. *Epsilonproteobacteria* occurred only at very low levels (0.01%~1.69%) in most bioactive wells, apart from FW026-R (7.19%). Additionally, the abundance of Gamma-*Proteobacteria* increased while Delta-*Proteobacteria* decreased significantly after the long-term groundwater invasion (Table S2, P-value < 0.05).

At the class and order levels, the major composition of *Firmicutes* was unique in 101-2-O and 101-2-R; it consisted mainly of the *Clostridia* class and the *Clostridiales* order, which accounted for more than 90% of the total *Firmicutes* community. Nevertheless, at the family level, signs appeared of a divergence of the *Firmicutes* composition between 101-2-O and 101-2-R. *Peptococcaceae 1* and *Clostridiaceae 1* were the dominant families and contributed 65.9% and 26.9% of *Firmicutes* in 101-2-O, whereas *Peptococcaceae 1* and *Peptococcaceae 2* were the dominant families and accounted for 54.6% and 31.2% of *Firmicutes* in 101-2-R, respectively. At the genus level, 101-2-R and 101-2-O shared *Desulfosporosinus* as the most abundant genus that could be classified. After *Desulfosporosinus*, *Clostridium sensu stricto* was the next most dominant composition for *Firmicutes* in 101-2-O.

Similar phenomenon was also found for *Acidobacteria* in the sample of 104-O and 104-R. That is, both the abundance and the composition of *Acidobacteria* altered greatly after the long-term groundwater invasion (Figure S6 and Figure S7). *Acidobacteria* was the predominant phylum, accounting for as much as 60.2% of the bacteria in 104-O; it was much less abundant in the counterpart 104-R (20.0%). At the class level, *Holophagae* and *Acidobacteria_Gp16* were dominant and accounted for 88.8% and 9.82%, respectively, of the *Acidobacteria* in 104-R. *Holophagae* and *Acidobacteria_Gp23* were abundant and accounted for 78.2% and 16.4%, respectively, of the *Acidobacteria* in 104-O. The composition ratio of *Holophagae* remained relatively constant during the bioreduction and reoxidation stages in FW104. At the genus level, *Gp16* and *Gp23* were the most abundant genera that could be classified and accounted for 9.82% and 16.4% of the *Acidobacteria* in 104-R and 104-O, respectively.

S3 U(VI)-reducing genera

Geobacter, the important Fe(III)- and U(VI)-reducing genus whose growth was promoted significantly via acetate or ethanol bioremediation in field experiments, was found at uranium-contaminated sites located in both Rifle, Colorado, and Oak Ridge, Tennessee, USA (Mouser et al., 2009, Van Nostrand et al., 2011, Wu et al., 2010, Zhuang et al., 2011). This dissimilatory metal-reducing bacteria could limit uranium toxicity by reducing soluble U(VI) to insoluble U(IV). It has been reported that the conductive pili of *Geobacter* function as sites of U(VI) reduction and prevent its accumulation in the periplasm (Cologgi et al., 2011). Previous study also found the similar variation pattern of *Geobacter,* that is, the abundance of *Geobacter* decreased drastically after the inner loop exposed to the source zone groundwater containing high concentration of nitrate for about 3 months (Wu et al., 2010).

Anaeromyxobacter，the U(VI) reducer found in both sediments and groundwater at the ORFRC (Cardenas et al., 2010, Thomas et al., 2009, Van Nostrand et al., 2011), can also use several other electron acceptors, including nitrate, Fe(III), and chlorinated hydrocarbons (He and Sanford 2003, Rooney-Varga et al., 1999). It was reported that microorganisms with the ability to use multiple FRC contaminants as electron donors or acceptors were able to outcompete other microorganisms in the acidic subsurface (North et al., 2004). *Acidovorax,* the denitrifying bacteria, could reduce U(VI) to U(IV) using acetate, ethanol, and aromatic compounds as electron donors in the uranium-contaminated subsurface. Nitrate has been shown to be able to reoxidize and remobilize Fe(III) (Senko et al., 2002), and the presence of this denitrifier could contribute to the removal of the competing electron acceptors and guarantee the stability of the reduced uranium (Cardenas et al., 2008). That might be the key reason for the increase of relative abundance of *Acidovorax* (P-value<0.05) after the long-term groundwater invasion containing high concentration of nitrate.

Sulfate-reducing bacteria (SRB) played key roles in both direct (enzymatic) and indirect (abiotic) U(VI) reduction (Van Nostrand et al., 2011). It was reported that sulfate in the treated area supported the growth of U(VI)-reducing SRB and facilitated U(VI) reduction (Xu et al., 2010). The main SRB identified to date at the ORFRC site and Rifle-FRC site were *Desulfovibrio* and *Desulfosporosinus* (Cardenas et al., 2010, Van Nostrand et al., 2009, Van Nostrand et al., 2011, Xu et al., 2010). *Desulfovibrio* might be a primary microorganism reducing U(VI) and a nearly ubiquitous SRB capable of bio-transforming U(VI) to U(IV) in bicarbonate buffers (Nyman et al., 2006). Compared with *Desulfovibrio, Desulfosporosinus* were considered to play a minor role in U(VI) reduction but a bigger role in the long-term stability of the reduced uranium, as they can form spores and survive under starvation conditions (Cardenas et al., 2008). Similar to *Geobacter*, *Desulfosporosinus* could also reduce As (V) apart from U(VI) reduction (Giloteaux et al., 2013). In addition, some *Desulfosporosinus* spp. were able to tolerate the high-salinity pressure in subsurface sediments stimulated for U(VI) reduction (Nevin et al., 2003).

Ferribacterium, one representative Fe(III)-reducing bacterium was associated with U(VI) reduction mainly because of its indirect (abiotic) U(VI) reduction (Cardenas et al., 2010). *Clostridium* are ubiquitous in soils, sediments, and wastes and could be very useful in the pretreatment and stabilization of uranium in radioactive wastes or at the corresponding contaminant sites (Francis et al., 1994, Madden et al., 2007, Suzuki et al., 2003).

S4 Co-occurrence and co-exclusion patterns among microbial taxa and environmental parameters

Figure 5 consists of 58 nodes (53 microbial taxa and 5 environmental parameters) and 150 edges. Some topological properties widely used in network analysis were calculated to describe the complex pattern of interrelationships among microbial taxa and environmental variables. The average degree or node connectivity was 5.172. The average network distance between all pairs of nodes, i.e., average path length, was 5.04 edges with a network diameter of 12 edges. The clustering coefficient (that is, how nodes are embedded in their neighborhood and thus the degree to which they tend to cluster together) was 0.509, and the modularity index was 0.478 (values >0.4 suggest that the network has a modular structure; Newman, 2006).

Figure S10 visualizes the significantly negative correlations (79 edges) among 34 bacterial genera and 5 environmental parameters. Some topological properties commonly used in network analysis were summarized as follows. The average degree was 4.051 and average network distance between all pairs of nodes was 2.868 edges with a network diameter of 7 edges. By contrast, the negative correlations, which reflect genus–genus or genus–environmental variable exclusion patterns, tend to be unclustered (an average clustering coefficient of 0) and unmodularized (modularity: −0.044), compared with the highly clustered, more modularized (modularity: 0.586) positive correlations (Figure 5), revealing distinct characteristics of positive and negative interactions among microbial genera and environmental variables.

Table S1. Diversity comparison before and after long-term groundwater invasion

	Sample	Reads		Richness [c]			Evenness [c]	Diversity [c]
		Raw reads	[a] Effective reads after normalization	OTUs	chao1	ACE	Buzas and Gibson's evenness	Shannon
Inner loop-Reoxidized	104-O	31939	5364	433	735	781	0.27	4.78
	101-1-O	11698	5364	408	797	818	0.41	5.12
	101-2-O	21915	5364	418	739	777	0.55	5.43
	101-3-O	12538	5364	526	1004	1006	1.17	6.42
	101-4-O	21680	5364	432	770	824	0.42	5.21
	102-1-O	12398	5364	998	2004	2137	2.09	7.54
	102-2-O	6625	5364	848	1497	1618	1.23	6.95
	102-3-O	23050	5364	921	1840	2023	2.03	7.53
	102-4-O	27989	5364	955	2029	2048	2.03	7.57
	026-O	19956	5364	454	853	820	0.64	5.67
Inner loop-Bioreduced	104-R	6671	5364	515	1039	1121	0.77	5.98
	101-2-R	6769	5364	481	905	965	0.94	6.11
	101-3-R	6458	5364	599	1274	1296	1.39	6.73
	101-4-R	5450	5364	971	1997	2034	2.19	7.66
	102-1-R	8566	5364	1091	2720	2722	1.83	7.60
	102-2-R	8883	5364	982	1978	1975	2.96	7.98
	102-3-R	5954	5364	533	952	1031	1.12	6.39
	102-4-R	7118	5364	638	1303	1407	0.88	6.34
	026-R	6188	5364	526	876	918	0.81	6.06
Outer loop-Reoxidized	024-O	13832	5364	507	831	878	1.64	6.73
	100-1-O	16234	5364	238	549	645	0.06	2.64
	100-2-O	5799	5364	273	422	442	0.24	4.18
	100-3-O	11011	5364	442	741	744	0.38	5.14
	100-4-O	17528	5364	285	720	645	0.13	3.58
Outer loop-Bioreduced	100-2-R[b]	2050	—	—	—	—	—	—
	100-3-R	5564	5364	713	1390	1421	1.46	6.95
	100-4-R	5451	5364	1169	2263	2467	2.32	7.90
	024-R	8121	5364	378	645	655	0.26	4.60
Downgradient well-Reoxidized	105-O	14282	5364	625	1423	1666	0.22	4.93
Downgradient well-Bioreduced	105-R	6889	5364	585	1187	1139	0.71	6.03

[a] As the number of sequences from 101-4-R is the smallest among the 29 samples (except for 100-2-R), to guarantee the same sequencing depth after denoise and chimera removal, 5,364 sequences randomly subsampled from each other sample were used to conduct the α-diversity analysis.

[b] Since the number of effective reads after denoise and chimera removal for sample of 100-2-R is 1970, much less than 5,364, 100-2-R was excluded during the calculation of richness, evenness and diversity.

[c] The species richness, evenness, and diversity index were calculated with a 3% distance cutoff.

Table S2. Abundance shift of subdivision of *Proteobacteria* after long-term groundwater invasion

Subdivision of *Proteobacteria*	Abundance at bioreduction stage (%)							Abundance at reoxidation stage (%)							P-values [a]
	101-2-R	101-3-R	102-2-R	102-3-R	104-R	026-R	Average	101-2-O	101-3-O	102-2-O	102-3-O	104-O	026-O	Average	
Alpha-	3.37	6.35	8.64	5.46	7.08	2.99	5.65	6.02	3.19	11.9	13.7	6.09	4.38	7.54	0.145
Beta-	4.08	13.8	12.0	11.0	16.1	8.66	10.9	22.9	20.5	32.3	15.9	7.15	17.2	19.3	0.056
Gamma-	4.90	5.28	7.06	15.1	4.24	2.88	6.57	7.59	13.7	14.8	18.0	5.30	8.42	11.3	**0.006**
Delta-	12.4	7.70	8.45	13.1	5.53	3.72	8.49	2.28	2.95	0.94	4.26	1.70	5.14	2.88	**0.011**
Epsilon-	0.65	1.78	0.28	0.18	1.69	7.19	1.96	0.01	0.03	0.21	0.04	0.01	0.03	0.05	0.071

[a] P-value refers to the one-tailed probability value of the paired t-test that was conducted to compare differentials in the abundance of *Proteobacteria* subdivision before and after long-term groundwater invasion.

Table S3. Abundance shift of U(VI)-reducing genera between active wells and inactive wells

U(VI)-reducing genera	Bio-reduced stage			Re-oxidized stage		
	Average abundance at active wells (%, n=6)	Average abundance at inactive wells (%,n=8)	P-values [a]	Average abundance at active wells (%, n=6)	Average abundance at inactive wells (%, n=10)	P-values [a]
Geothrix	2.24	0.74	**0.020**	0.69	0.27	0.19
Desulfosporosinus	3.15	0.44	**0.044**	11.7	0.85	**0.035**
Acidovorax	0.008	0.014	0.48	0.31	0.21	0.56
Anaeromyxobacter	0.57	0.013	**0.00031**	0.79	0.17	0.086
Desulfovibrio	6.10	0.16	**0.00045**	0.29	0.10	0.14
Geobacter	1.22	0.19	**0.030**	0.17	0.05	0.19
Ferribacterium	2.58	0.22	**0.018**	0.10	0.02	0.079
Clostridium-III	0.18	0.13	0.56	0.17	0.19	0.85
Clostridium-sensu-stricto	0.38	1.07	0.55	3.30	3.03	0.88
Clostridium-XI	0.18	0.35	0.45	0.12	0.33	0.36
Clostridium-XlVa	0.02	0.04	0.55	0.11	0.25	0.38

[a] P-value refers to the two-tailed probability value of the t-test that was conducted to compare differentials in the abundance of U(VI)-reducing genera between active wells and inactive wells.

Table S4. Summary of canonical correspondence analysis results

Axes	Axis 1	Axis 2
Percent variation explained	37.7%	22.5%
Eigenvalues	0.690	0.412
pH	−0.564	−0.019
Sulfate	0.222	0.428
Nitrate	0.681	0.028
U(VI)	0.345	0.456
Fe	0.468	0.234
DO	0.182	0.348
Cl	0.591	0.116
Al	0.390	-0.032
Ca	0.627	0.036
Mg	0.676	0.033
Mn	0.734	0.265

Table S5. Co-occurring microbial genera of module hub

Module ID of hub	Module hub	Co-occurring microbial genera	Module ID of co-occurring microbial genera	Category of co-occurring microbial genera
I	*Aquicella*	*Gemmatimonas*	I	Others
		Mycobacterium	III	Indicator genera at bioreduction stage
		Subdivision3_genera_incertae_sedis	I	Others
		Legionella	III	Others
		OD1_genera_incertae_sedis	I	Others
		Opitutus	I	Others
		Nocardioides	I	Others
		Sediminibacterium	I	Others
		Sulfuricurvum	I	Indicator genera at bioreduction stage
		Arthrobacter	III	Indicator genera at bioreduction stage
		Gp6	I	Indicator genera at bioreduction stage
		Phenylobacterium	I	Others
		Singulisphaera	III	Others
		Desulfobulbus	IV	Others
		Ferribacterium	III	U-reducing genera; indicator genera at bioreduction stage
		Parachlamydia	III	Indicator genera at bioreduction stage
II	*Castellaniella*	*Simplicispira*	II	Indicator genera at reoxidation stage
		Mesorhizobium	II	Others
		Bacillus	V	Others
		Polaromonas	II	Others
		Thermomonas	II	Others

Table S6. The co-occurring genera shared by hubs of Module I and Module III

Module ID	Hub	Co-occurring genera	Spearman's correlation coefficient ρ	The co-occurring genera shared by *Aquicella* and *Legionella*
I	*Aquicella*	*Gemmatimonas*	0.75	***Arthrobacter*** ***Ferribacterium*** ***Gemmatimonas*** ***Gp6*** ***Mycobacterium*** ***Parachlamydia*** ***Phenylobacterium*** ***Sediminibacterium*** ***Singulisphaera*** ***Sulfuricurvum***
		Mycobacterium	0.73	
		Subdivision3_genera_incertae_sedis	0.75	
		Legionella	0.80	
		OD1_genera_incertae_sedis	0.65	
		Opitutus	0.64	
		Nocardioides	0.69	
		Sediminibacterium	0.68	
		Sulfuricurvum	0.69	
		Arthrobacter	0.66	
		Gp6	0.83	
		Phenylobacterium	0.78	
		Singulisphaera	0.72	
		Desulfobulbus	0.64	
		Ferribacterium	0.62	
		Parachlamydia	0.71	
III	*Legionella*	*Gemmatimonas*	0.67	
		Mycobacterium	0.60	
		Aquicella	0.80	
		Arthrobacter	0.69	
		Ferribacterium	0.65	
		Gp6	0.72	
		Parachlamydia	0.76	
		Phenylobacterium	0.63	
		Sediminibacterium	0.64	
		Singulisphaera	0.71	
		Sulfuricurvum	0.64	

Table S7. The associations between environmental parameters and genera

Environmental factors	Co-excluding genera	ρ	Co-occurring genera	ρ
Nitrate	*Geothrix*	−0.66	*Simplicispira*	0.71
	Mycobacterium	−0.80	*Mesorhizobium*	0.61
	Legionella	−0.70	*Castellaniella*	0.84
	Sediminibacterium	−0.66	*Thermomonas*	0.62
	Arthrobacter	−0.69	—	—
	Desulfovibrio	−0.63	—	—
	Gp6	−0.64	—	—
	Phenylobacterium	−0.71	—	—
	Singulisphaera	−0.62	—	—
	Aquicella	−0.77	—	—
	Parachlamydia	−0.74	—	—
	Ferribacterium	−0.80	—	—
	Desulfobulbus	−0.72	—	—
pH	*Clostridium-sensu-stricto*	−0.65	*Gemmatimonas*	0.62
	Clostridium-XlVa	−0.68	*Legionella*	0.62
	Psychrosinus	−0.65	*Gp6*	0.65
Sulfate	*Azoarcus*	−0.72	—	—
Fe	*Mycobacterium*	−0.64	—	—
	Sediminibacterium	−0.65	—	—
	Singulisphaera	−0.63	—	—
U-VI	*Gemmatimonas*	−0.68	*Castellaniella*	0.65
	Mycobacterium	−0.60	*Rhizomicrobium*	0.73
	Subdivision3_genera_incertae_sedis	−0.65	—	—
	Legionella	−0.69	—	—
	Sulfuricurvum	−0.65	—	—
	Arthrobacter	−0.64	—	—
	Gp6	−0.74	—	—
	Phenylobacterium	−0.69	—	—
	Aquicella	−0.75	—	—
	Ferribacterium	−0.71	—	—
	Desulfobulbus	−0.66	—	—

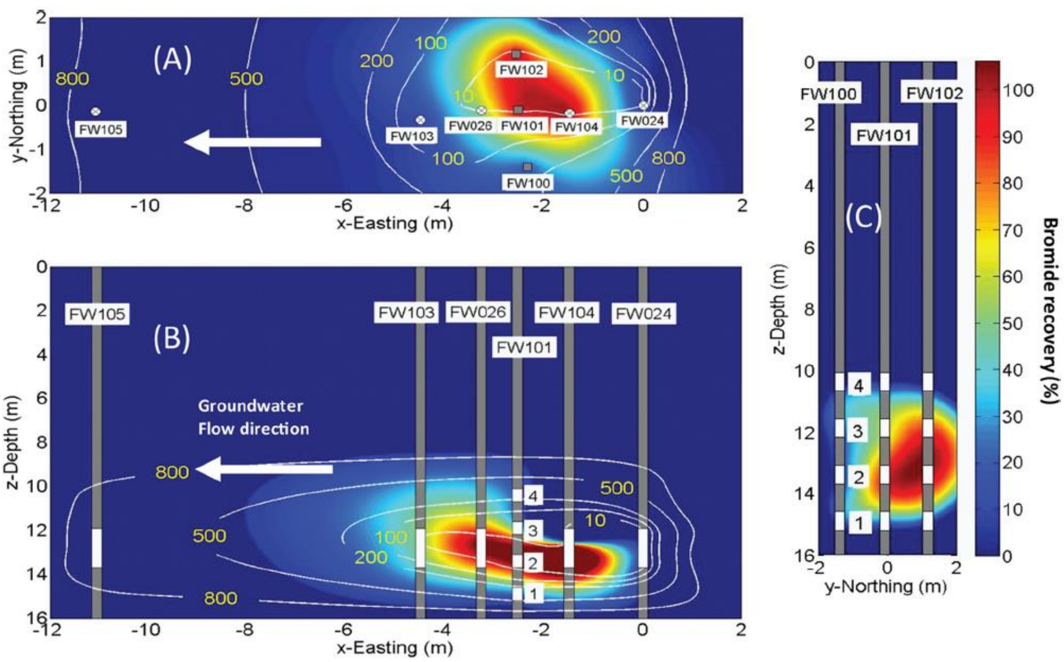

Figure S1. Scheme of the well system in Area 3, Oak Ridge National Laboratory, DOE. Hydrology connectivity is shown with the spatial distributions of bromide recovery (as percentage, in color) and mean travel times (contour lines with units of hours).
(A) Horizontal plane at the 13 m depth below ground;
(B) Cross-vertical section along injection and extraction wells;
(C) Cross-vertical section along MLS wells.
The horizontal distance (m) is measured from outer-loop injection well FW024 eastward (x) or northward (y). z is the depth below ground (m). The well system included inner-loop injection well FW104 and extraction well FW026 for ethanol injection, outer-loop injection well FW024 and extraction well FW103 for hydraulic protection, and downgradient well FW105. The multilevel sample wells are FW100, FW101, and FW102; and the -1, -2, -3, and -4 levels were used for monitoring. The electron donor (ethanol) was injected into the inner loop at well FW104.

Note: Figure S1 (A), (B) and (C) were extracted from our previous study (Cardenas et al., 2010). All the rights related to Figure S1 (A), (B) and (C) are reserved by American Society for Microbiology.

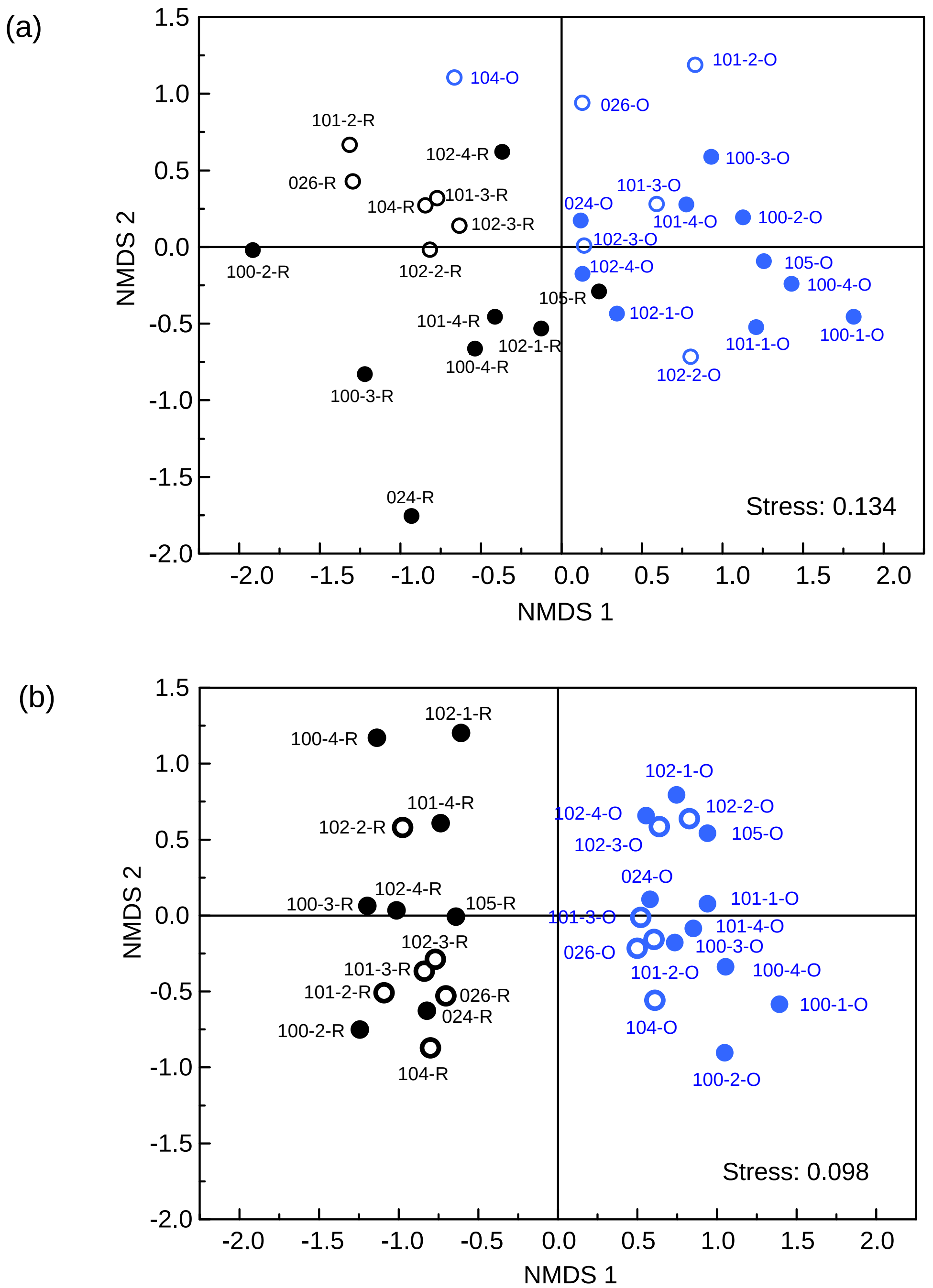

Figure S2. NMDS plot showing the microbial community differences (at 3% cutoff-OTU level) for all the selected wells before and after the long-term invasion of groundwater. Pairwise community distances were determined using (a) weighted UniFrac algorithm (b) unweighted UniFrac algorithm. Black and blue colors represent the samples collected from the bioreduction and reoxidation stages, respectively. Solid circles represent inactive wells and empty circles represent active wells classified according to the bromide recovery ratios during the bioreduction stage.

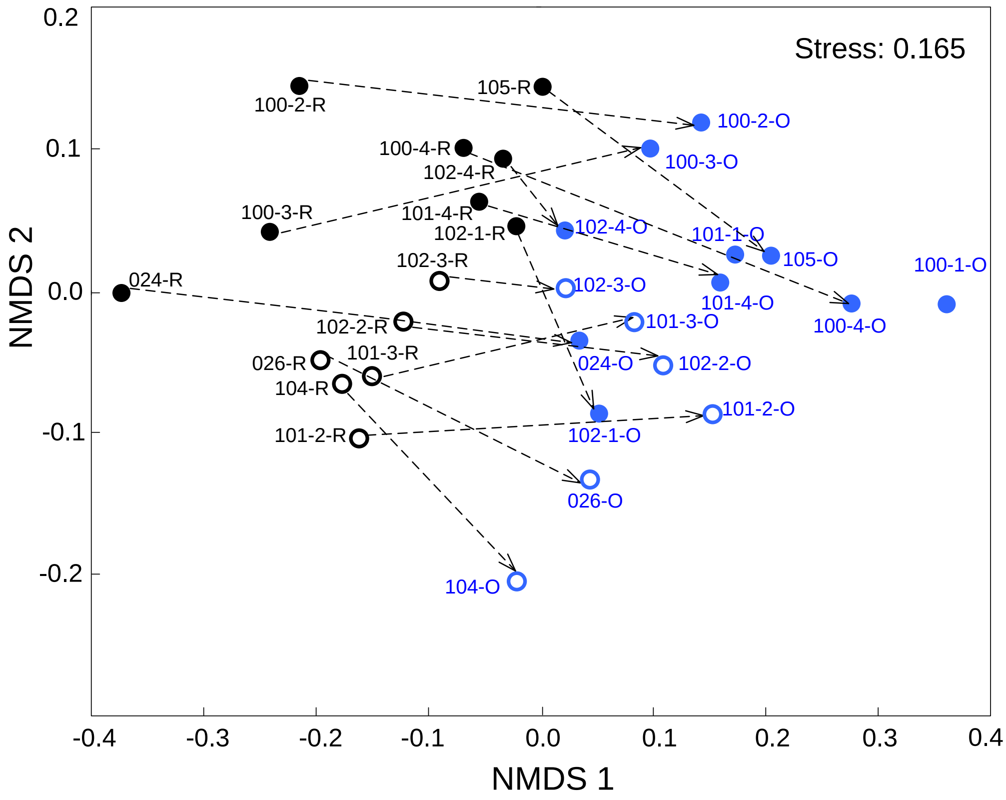

Figure S3. NMDS plot showing the microbial community shift (at genus level) for all the selected wells before and after the long-term invasion of groundwater. Black and blue colors represent the samples collected from the bioreduction and reoxidation stages, respectively. Solid circles represent inactive wells and empty circles represent active wells classified according to the bromide recovery ratios during the bioreduction stage. The dashed lines with arrows indicate the coordinate position shift of each specific sample in the NDMS plot.

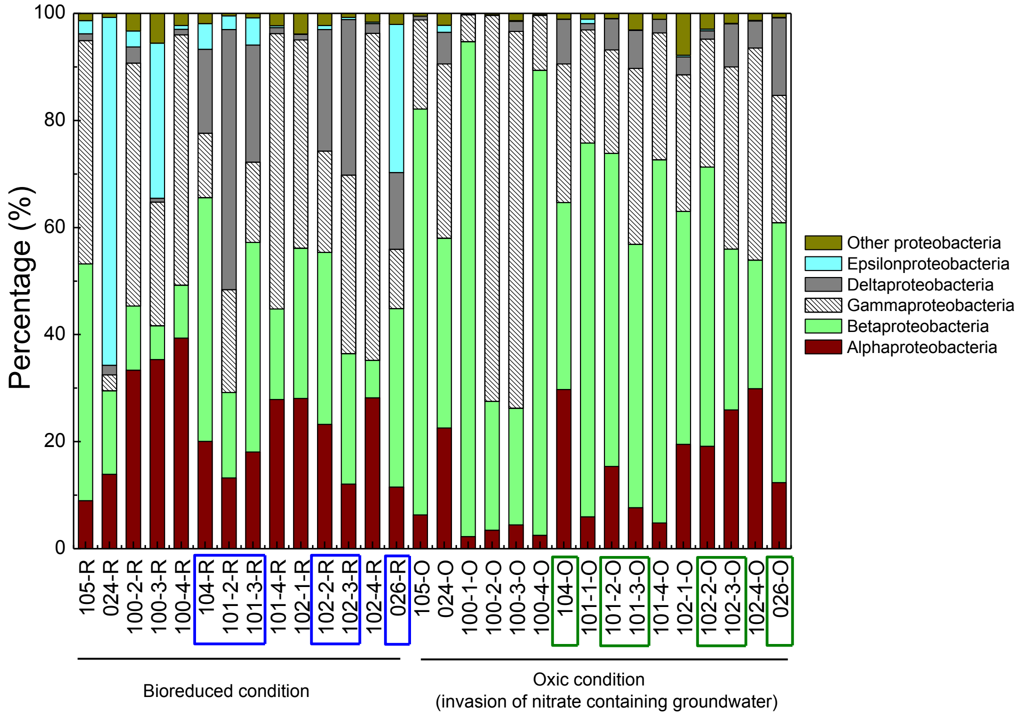

Figure S4. *Proteobacteria* composition at class level of samples during the bioreduction and reoxidation stages.

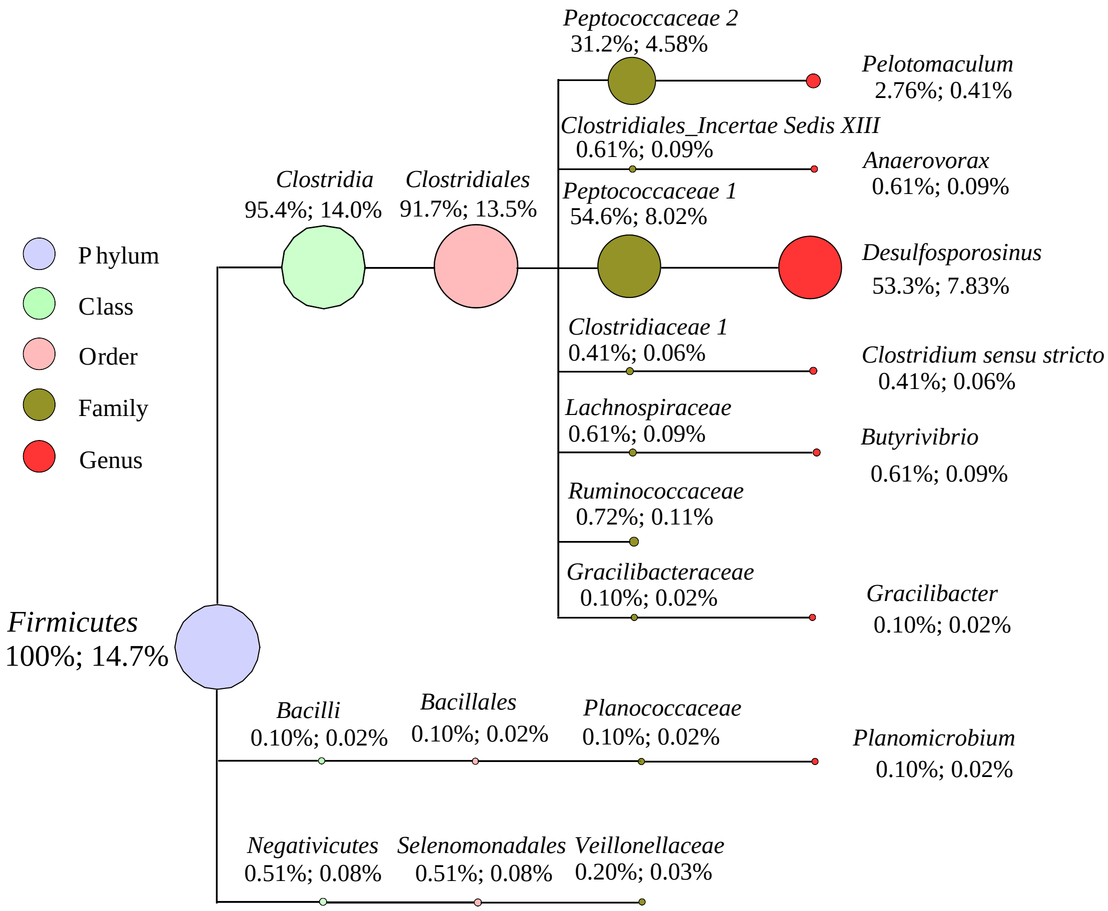

Figure S5. *Firmicutes* composition in sample of 101-2-R. The numbers after the taxonomic ranks are the abundance ratios of the corresponding taxons in the phylum of *Firmicutes* and sample of 101-2-R, respectively.

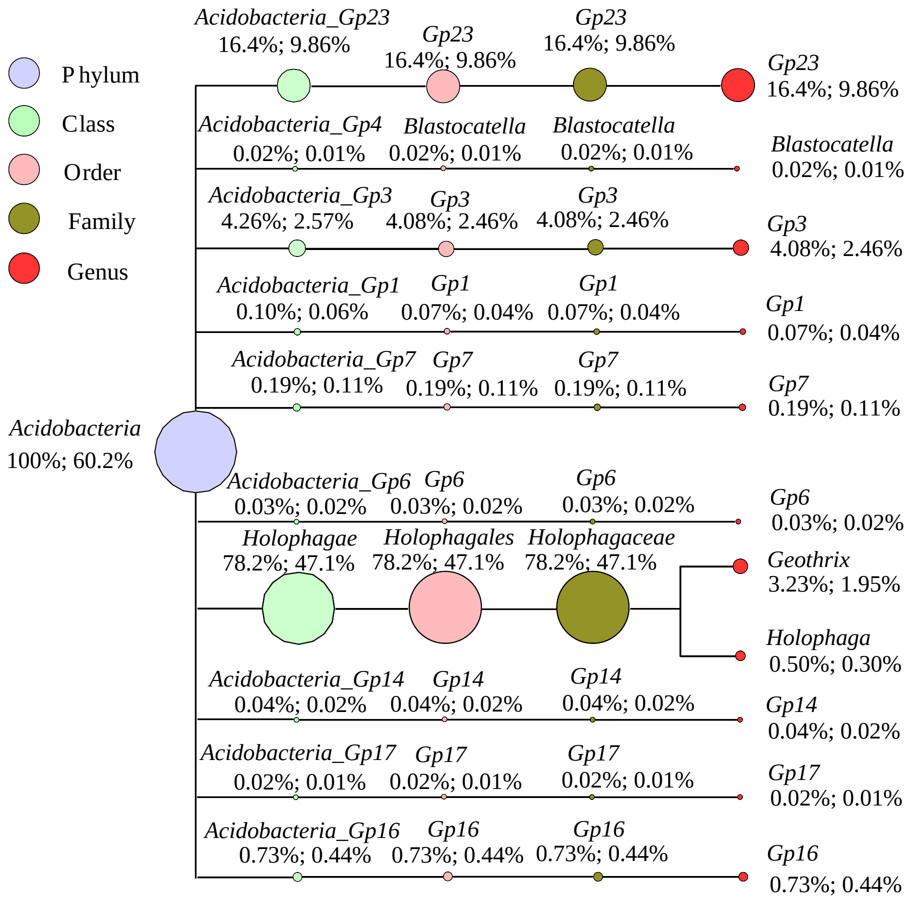

Figure S6. *Acidobacteria* composition in sample of 104-O. The numbers after the taxonomic ranks are the abundance ratios of the corresponding taxons in the phylum of *Acidobacteria* and sample of 104-O, respectively.

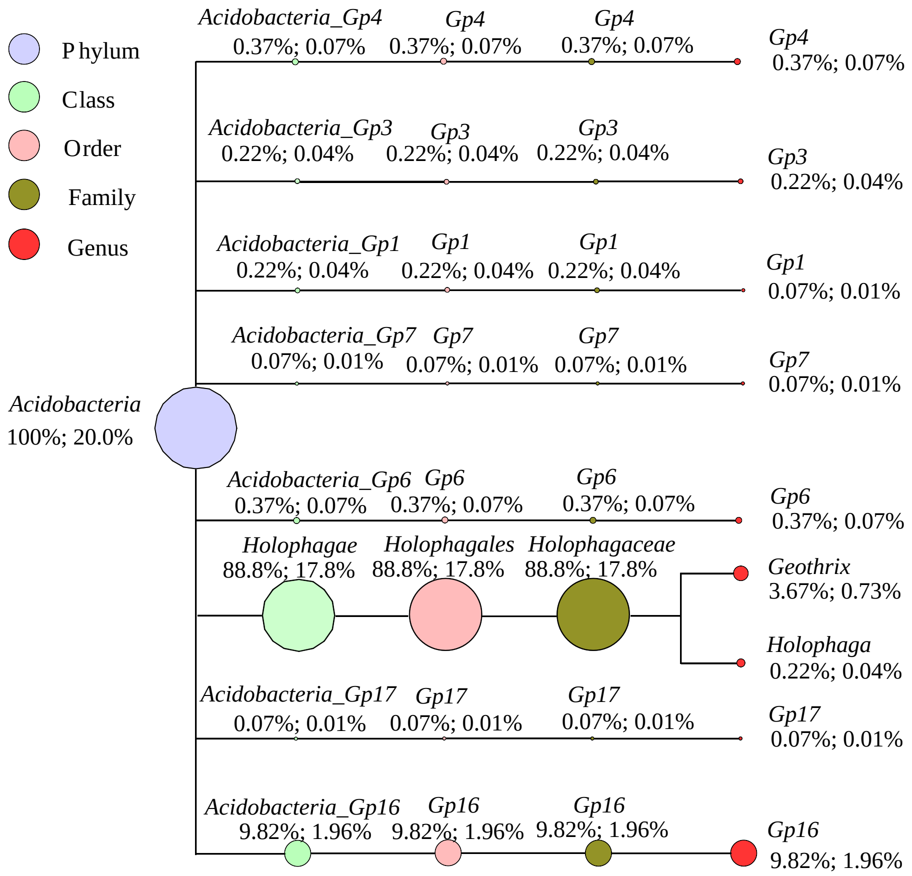

Figure S7. *Acidobacteria* composition in sample of 104-R. The numbers after the taxonomic ranks are the abundance ratios of the corresponding taxons in the phylum of *Acidobacteria* and 104-R, respectively.

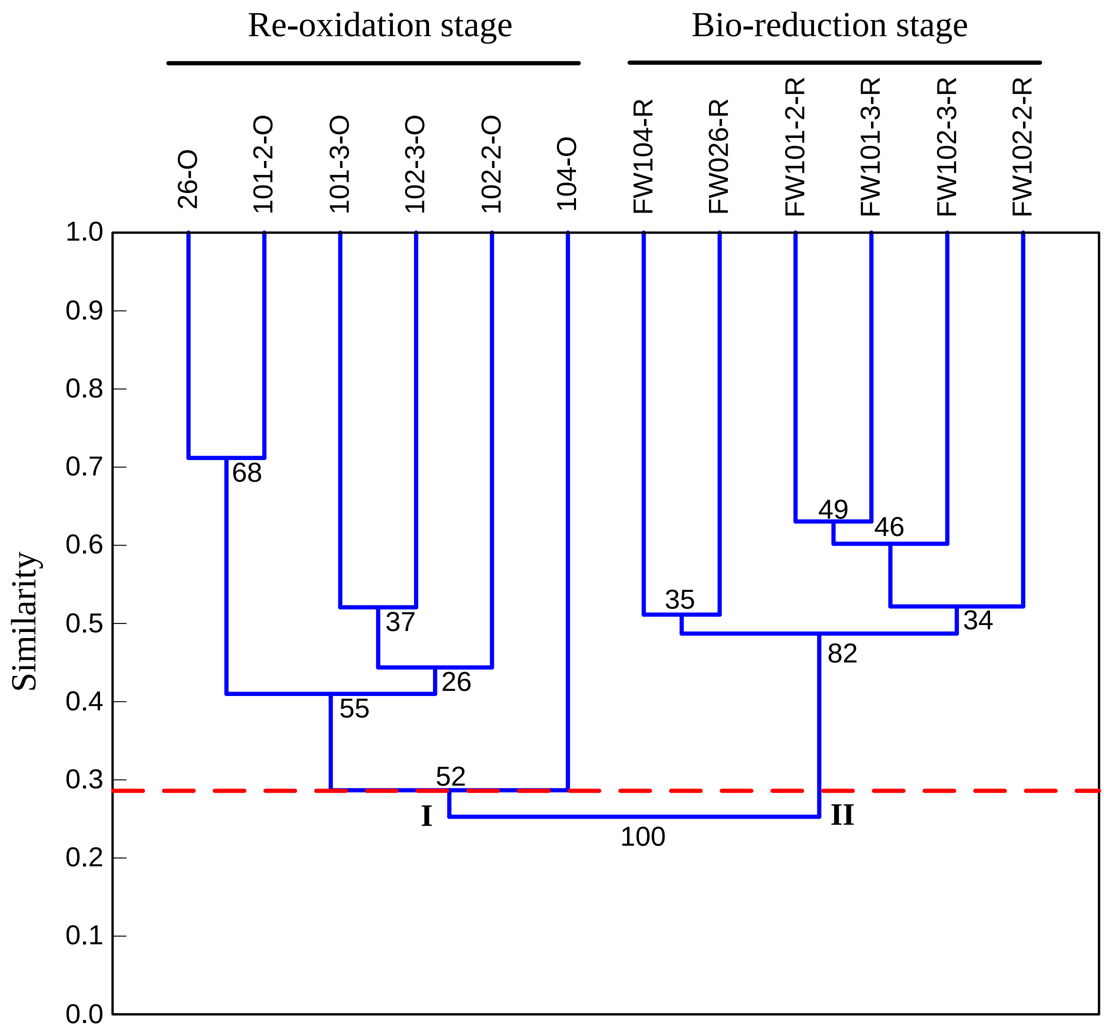

Figure S8. Cluster analysis (CA) of bacterial profiles in active wells before and after the long-term invasion of groundwater. CA was conducted based on the Bray-Curtis distance calculated from the matrix of genus relative abundance using PAST software. Unweighted pair group mean average (UPGMA) was selected as the algorithm for CA.

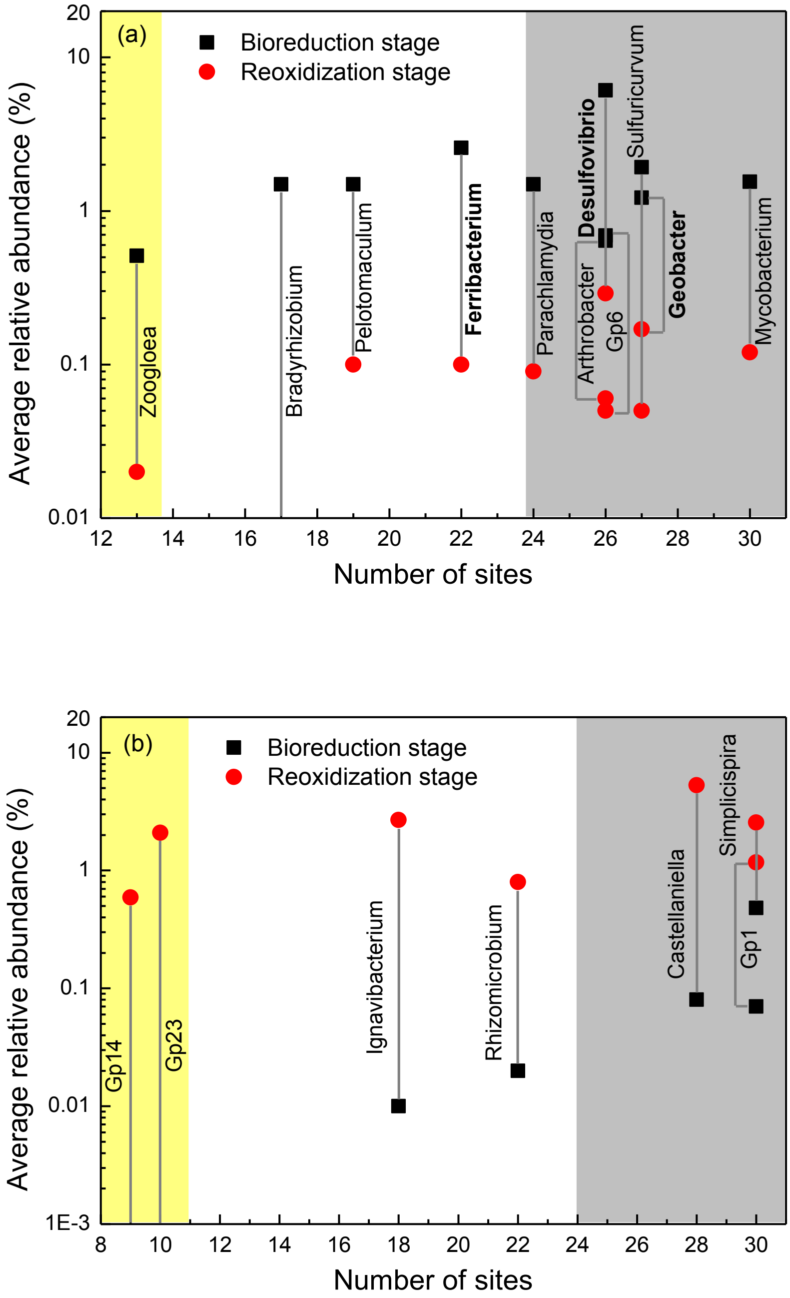

Figure S9. Average relative abundance (y-axis) and occupancy (x-axis) of indicator genera at (a) bioreduction stage and (b) reoxidization stage. The genera located in the shaded area (gray color) belong to persistent genera with occupancies ⩾80% (24 samples). The genera located in the shaded area (yellow color) belong to specialist genera with low occupancies ⩽45% (13 samples).The genera marked with bold font are U(VI)-reducing genera.

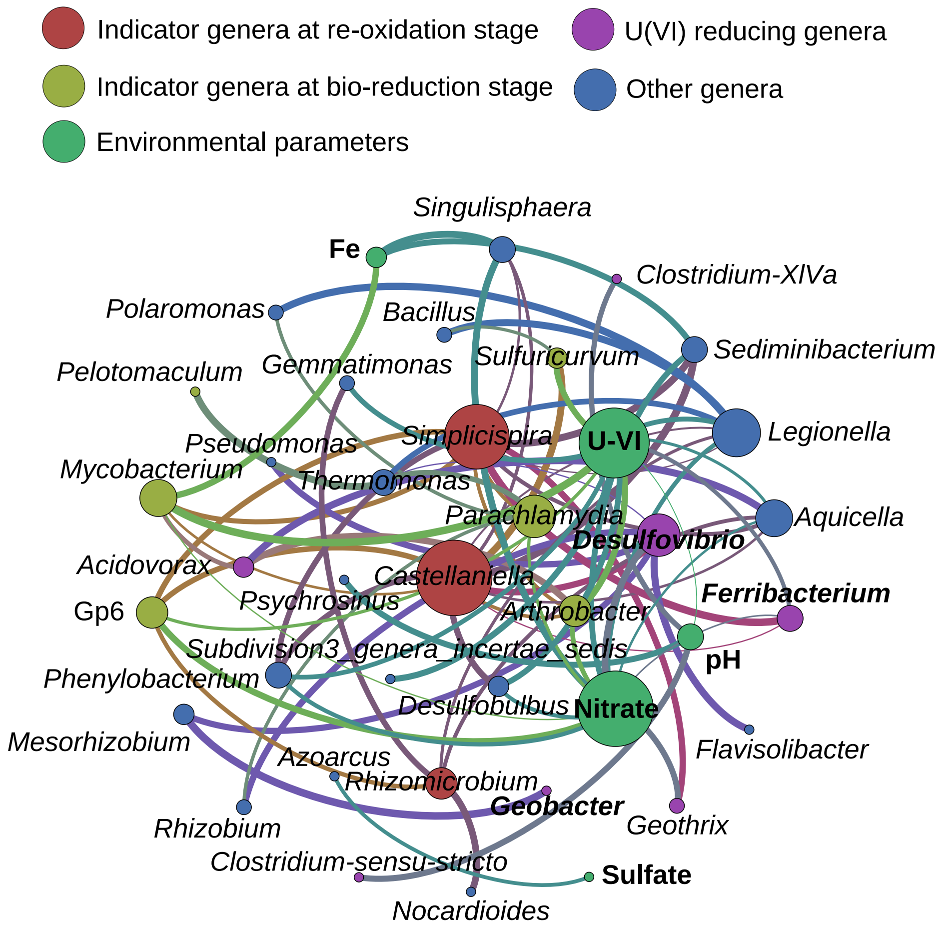

Figure S10. The network analysis revealing the co-exclusion patterns among microbial taxa and environmental parameters. The nodes were colored according to functional taxa and environmental parameters. A connection represents a strongly (Spearman's correlation coefficient $\rho<-0.6$) and significantly (P-value <0.01) negative correlation. The size of each node is proportional to the number of connections, i.e., the degree. Three U(VI)-reducing genera, *Geobacter*, *Desulfovibrio*, and *Ferribacterium* (marked with bold font), are also indicator genera at the bioreduction stage.

References:

Steele JA, Countway PD, Xia L, Vigil PD, Beman JM, Kim DY *et al.*, (2011). Marine bacterial, archaeal and protistan association networks reveal ecological linkages. *Isme J* **5:** 1414–1425.

Benjamini Y, Hochberg Y (1995). Controlling the false discovery rate—A practical and powerful approach to multiple testing. *Journal of the Royal Statistical Society Series B-Methodological* **57:** 289–300.

Mouser PJ, Holmes DE, Perpetua LA, DiDonato R, Postier B, Liu A *et al.*, (2009). Quantifying expression of Geobacter spp. oxidative stress genes in pure culture and during in situ uranium bioremediation. *Isme J* **3:** 454–465.

Van Nostrand JD, Wu LY, Wu WM, Huang ZJ, Gentry TJ, Deng Y et al., (2011). Dynamics of microbial community composition and function during in situ bioremediation of a uranium-contaminated aquifer. *Applied and Environmental Microbiology* **77:** 3860–3869.

Wu WM, Carley J, Green SJ, Luo J, Kelly SD, Van Nostrand J *et al.*, (2010). Effects of nitrate on the stability of uranium in a bioreduced region of the subsurface. *Environmental Science & Technology* **44:** 5104–5111.

Zhuang K, Izallalen M, Mouser P, Richter H, Risso C, Mahadevan R *et al.*, (2011). Genome-scale dynamic modeling of the competition between Rhodoferax and Geobacter in anoxic subsurface environments. *Isme J* **5:** 305–316.

Cologgi DL, Lampa-Pastirk S, Speers AM, Kelly SD, Reguera G (2011). Extracellular reduction of uranium via Geobacter conductive pili as a protective cellular mechanism. *P Natl Acad Sci USA* **108:** 15248–15252.

Xu MY, Wu WM, Wu LY, He ZL, Van Nostrand JD, Deng Y *et al.*, (2010). Responses of microbial community functional structures to pilot-scale uranium in situ bioremediation. *Isme J* **4:** 1060–1070.

Cardenas E, Wu WM, Leigh MB, Carley J, Carroll S, Gentry T *et al.*, (2010). Significant association between sulfate-reducing bacteria and uranium-reducing microbial communities as revealed by a combined massively parallel sequencing-indicator species approach. *Applied and Environmental Microbiology* **76:** 6778–6786.

Van Nostrand JD, Wu WM, Wu LY, Deng Y, Carley J, Carroll S *et al.*, (2009). GeoChip-based analysis of functional microbial communities during the reoxidation of a bioreduced uranium-contaminated aquifer. *Environmental Microbiology* **11:** 2611–2626.

Nyman JL, Marsh TL, Ginder-Vogel MA, Gentile M, Fendorf S, Criddle C (2006). Heterogeneous response to biostimulation for U(VI) reduction in replicated sediment microcosms. *Biodegradation* **17:** 303–316.

Cardenas E, Wu WM, Leigh MB, Carley J, Carroll S, Gentry T *et al.*, (2008). Microbial communities in contaminated sediments, associated with bioremediation of uranium to submicromolar levels. *Applied and Environmental Microbiology* **74:** 3718–3729.

Giloteaux L, Holmes DE, Williams KH, Wrighton KC, Wilkins MJ, Montgomery AP *et al.*, (2013). Characterization and transcription of arsenic respiration and resistance genes during in situ uranium bioremediation. *Isme J* **7:** 370–383.

Nevin KP, Finneran KT, Lovley DR (2003). Microorganisms associated with uranium bioremediation in a high-salinity subsurface sediment. *Applied and Environmental Microbiology* **69:** 3672–3675.

Francis AJ, Dodge CJ, Lu FL, Halada GP, Clayton CR (1994). XPS and XANES studies of uranium reduction by Clostridium sp.. *Environmental Science & Technology* **28:** 636–639.

Madden AS, Smith AC, Balkwill DL, Fagan LA, Phelps TJ (2007). Microbial uranium immobilization independent of nitrate reduction. *Environmental Microbiology* **9:** 2321–2330.

Suzuki Y, Kelly SD, Kemner KA, Banfield JF (2003). Microbial populations stimulated for hexavalent uranium reduction in uranium mine sediment. *Applied and Environmental Microbiology* **69:** 1337–1346.